

EUR 3789 e

EUROPEAN ATOMIC ENERGY COMMUNITY — EURATOM

**STUDIES ON THE STEADY STATE
AND DYNAMIC BEHAVIOR
OF A BOILING WATER REACTOR**

Final Report

1968



Euratom/US Agreement for Cooperation

EURAEK Report No. 1996 prepared by the
Technological University of Eindhoven, Eindhoven - Netherlands

Euratom Contract No. 069-65-7 TEEN

LEGAL NOTICE

This document was prepared under the sponsorship of the Commission of the European Communities in pursuance of the joint programme laid down by the Agreement for Cooperation signed on 8 November 1958 between the Government of the United States of America and the European Communities.

It is specified that neither the Commission of the European Communities, nor the Government of the United States, their contractors or any person acting on their behalf :

Make any warranty or representation, express or implied, with respect to the accuracy, completeness, or usefulness of the information contained in this document, or that the use of any information, apparatus, method, or process disclosed in this document may not infringe privately owned rights; or

Assume any liability with respect to the use of, or for damages resulting from the use of any information, apparatus, method or process disclosed in this document.

This report is on sale at the addresses listed on cover page 4

at the price of FF 10.—	FB 100.—	DM 8.—	Lit. 1250	Fl. 7.25
-------------------------	----------	--------	-----------	----------

When ordering, please quote the EUR number and the title, which are indicated on the cover of each report.

Printed by Van Muysewinkel
Brussels, June 1968.

This document was reproduced on the basis of the best available copy.

EUR 3789 e

STUDIES ON THE STEADY STATE AND DYNAMIC BEHAVIOR OF A BOILING WATER REACTOR — Final Report

European Atomic Energy Community — EURATOM

EURATOM/US Agreement for Cooperation

EURAEK Report No. 1996 prepared by the Technological University of Eindhoven, Eindhoven (Netherlands)

Euratom Contract No. 069-65-7 TEEN

Brussels, June 1968 — 70 Pages — 23 Figures — FB 100

This report concludes the work carried out in the field of the steady state and stability characteristics of a two-phase flow. The contract started on July 1, 1965 and expired June 30, 1966. The writing of the final report has been postponed for one year in order to allow the inclusion of some recent results obtained after the expiration of the contract.

EUR 3789 e

STUDIES ON THE STEADY STATE AND DYNAMIC BEHAVIOR OF A BOILING WATER REACTOR — Final Report

European Atomic Energy Community — EURATOM

EURATOM/US Agreement for Cooperation

EURAEK Report No. 1996 prepared by the Technological University of Eindhoven, Eindhoven (Netherlands)

Euratom Contract No. 069-65-7 TEEN

Brussels, June 1968 — 70 Pages — 23 Figures — FB 100

This report concludes the work carried out in the field of the steady state and stability characteristics of a two-phase flow. The contract started on July 1, 1965 and expired June 30, 1966. The writing of the final report has been postponed for one year in order to allow the inclusion of some recent results obtained after the expiration of the contract.

Most of the results obtained from experiments during this period have been published earlier. In this report a short description of the experimental set-up and the instrumentation has been included.

A brief quotation from the thesis of Spigt (EUR 2842.e — EURAEC 1644) is inserted.

A description is given of a limited number of experiments, some of which have been carried out after the date of expiration of the contract.

Are also given the results of measurements carried out under natural circulation in order to investigate the influence of heating elements with different response characteristics on the stability of the system.

Preliminary measurements with forced convection are reported and compared with corresponding experiments under natural convection.

Finally a summary is given of the state of development of the theoretical models.

Most of the results obtained from experiments during this period have been published earlier. In this report a short description of the experimental set-up and the instrumentation has been included.

A brief quotation from the thesis of Spigt (EUR 2842.e — EURAEC 1644) is inserted.

A description is given of a limited number of experiments, some of which have been carried out after the date of expiration of the contract.

Are also given the results of measurements carried out under natural circulation in order to investigate the influence of heating elements with different response characteristics on the stability of the system.

Preliminary measurements with forced convection are reported and compared with corresponding experiments under natural convection.

Finally a summary is given of the state of development of the theoretical models.

EUR 3789 e

EUROPEAN ATOMIC ENERGY COMMUNITY — EURATOM

**STUDIES ON THE STEADY STATE
AND DYNAMIC BEHAVIOR
OF A BOILING WATER REACTOR**

Final Report

1968



Euratom/US Agreement for Cooperation

EURAEK Report No. 1996 prepared by the
Technological University of Eindhoven, Eindhoven - Netherlands

Euratom Contract No. 069-65-7 TEEN

Summary

This report concludes the work carried out in the field of the steady state and stability characteristics of a two-phase flow. The contract started on July 1, 1965 and expired June 30, 1966. The writing of the final report has been postponed for one year in order to allow the inclusion of some recent results obtained after the expiration of the contract.

Most of the results obtained from experiments during this period have been published earlier. In this report a short description of the experimental set-up and the instrumentation has been included.

A brief quotation from the thesis of Spigt (EUR 2842.e — EURAEC 1644) is inserted.

A description is given of a limited number of experiments, some of which have been carried out after the date of expiration of the contract.

Are also given the results of measurements carried out under natural circulation in order to investigate the influence of heating elements with different response characteristics on the stability of the system.

Preliminary measurements with forced convection are reported and compared with corresponding experiments under natural convection.

Finally a summary is given of the state of development of the theoretical models.

KEYWORDS

STABILITY
TWO-PHASE FLOW
INSTRUMENTS
NATURAL CIRCULATION
HEATING
PERFORMANCE
COOLANT LOOPS

Contents.

1	Introduction	9
2	Description of the set-ups	9
	2.1. The pressurized boiling water loop	10
	2.1.1. Power supply	11
3	Instrumentation	12
	3.1. Measuring equipment	12
	3.2. Recording equipment	15
	3.3. Analyzing equipment	17
4	Measurements	19
	4.1. Measurements with natural circulation	19
	4.2. Measurements with forced circulation	24
5	Theoretical studies	28
	5.1. Linearized model	28
	5.1.1. Introduction	28
	5.1.1.a. Summation of the energy equations	29
	5.1.1.b. Incorporation of a pump	29
	5.1.1.c. Incorporation of the dynamic characteristics of the heating element	30
	5.2. Basic principle model	41
6	Future program	43
7	References	44
	Figures	47

List of figures.

- Fig. 1. The longitudinal void fraction distribution for various channel powers, Test Section I.
- Fig. 2. Autocorrelations and spectral power densities of the Δp -inlet signal.
- Fig. 3. Void fraction data plotted according to Martinelli-Nelson for three system pressures, Test Section I.
- Fig. 4. Void fraction data plotted according to Zuber and Findlay for three system pressures, Test Section I.
- Fig. 5. Recordings of the signals from the various void gauges and the pitot-tube, Test Section I.
- Fig. 6. The influence of system pressure on the onset of hydraulic instabilities, Test Sections I and II.
- Fig. 7. Transfer functions from channel power to inlet mass flow for various channel powers, Test Section I.
- Fig. 8. Flowsheet of the pressurized boiling water loop.
- Fig. 9. The longitudinal pressure distribution at three channel powers for forced circulation and natural circulation.
- Fig. 10. a. Thresholds of instabilities from the signals of the pitot-tube and the void gauges, at forced circulation-inlet flowrate nearly zero.
- Fig. 10. b. Thresholds of instabilities from the signals of the pitot-tube and the void gauges at forced circulation, inlet flowrate 1,5 m/sec.
- Fig. 11. Recordings of the signals from the pitot-tube and various void gauges under forced circulation; saturation temperature 120°C, inlet flowrate nearly zero; ΔT sub. 0,5°C.
- Fig. 12. Recordings of the signals from the pitot-tube and various void gauges under forced circulation; saturation temperature 120°C, inlet flowrate 1,5 m/sec.
- Fig. 13. Transfer functions from channel power to inlet mass flow for various channel powers.
- Fig. 14. Transfer function from channel power to inlet mass flow at a constant frequency (0,9 Hz) and different power levels under forced circulation.

- Fig. 15. Transfer functions from channel power to the void fraction at different locations under forced circulation.
- Fig. 16. Transfer functions from channel power to the void fraction at different locations under natural circulation.
- Fig. 17. Approximated transfer functions of the electrically heated solid bar from equations (50), (52) and (53) compared with the exact solution.
- Fig. 18. Approximated transfer functions of the tube from equations (60), (61) and (64) compared with the exact solution.
- Fig. 19. Transfer function from channel power to inlet mass flow for different heating elements from a digital model of a boiling water system.
- Fig. 20. Transfer function from channel power to elongation of the heating element (solid bar) at three system pressures.
- Fig. 21. Transfer function from channel power to elongation for a solid bar and tube.
- Fig. 22. Transfer function from channel power to inlet mass flow for two channel powers and different heating elements.
- Fig. 23. Steady state results calculated by a theoretical study based on "first principles".

Nomenclature.

		dimension
a	$\frac{\lambda_m}{\rho_m c_m}$	$m^2 sec^{-1}$
A	cross section of heating element	m^2
B	defined in text - related to series expansion	$Nm^{-2} oC^{-1}$
B_1, B_2	constants in eq. 1	
c	specific heat	$Nmkg^{-1} oC^{-1}$
c_1, c_2, c_3	constants in pump characteristic	
D	defined in text-related to series expansion	m^{-2}
h	heat transfer coefficient	$Nm^{-1} oC^{-1} sec^{-1}$
J	Besselfunction	
k	pressure loss coefficient	
p	pressure	Nm^{-2}
Δp	pressure difference	Nm^{-2}
Q	heat input per unit length	$Nsec^{-1}$
Q'	heat input per unit length per unit flow area	$Nm^{-2} sec^{-1}$
r	radius	m
	heat of evaporation (with subscript s)	$Nmkg^{-1}$
t	time	sec
T	temperature	oC
u	$z \sqrt{\frac{i}{\sigma}}$	
v	velocity	$msec^{-1}$
Y	Besselfunction	
z	$\frac{r}{r_o}$	
Z	defined in text	

Greek symbols

α	void fraction
β	$\frac{u}{r_o}$
γ	slipfactor

δ	$\frac{2\pi r_o h}{\lambda_m}$	
z	length in axial direction	m
η	$\frac{r_i}{r_o}$	
θ	time constant - related to series expansion	sec
κ	heat distribution parameter in subcooled boiling	
λ	heat conduction coefficient	$N^{\circ}C^{-1}sec^{-1}$
ρ	specific weight	$kg.m^{-3}$
σ	$\frac{\lambda_m}{\rho_m c_m \omega r_o^2}$	
τ	time constant	sec
ω	circle frequency	sec^{-1}

Subscripts.

a	Q_a - heat passing the surface of the heating element
ci	channel inlet
f	fluid
i	unstable condition - related to physical quantities
	inner wall
m	material of heating element
n	limit variable
o	outer wall
s	solid bar - related to τ
	steam
t	tubular element
w	surface of element

STUDIES ON THE STEADY STATE AND DYNAMIC BEHAVIOR
OF A BOILING WATER REACTOR (+)

1. Introduction.

At the Technological University at Eindhoven a research program has been carried out to study the heat transfer and stability characteristics of a boiling water system under pressures up to 40 atm. A great deal of the research has been performed under contract with the EURATOM/ U.S.A. Joint Research and Development Board during an uninterrupted period of 5½ years, starting December 1st. 1960. This period can be divided into three parts:

December 1st. 1960	- December 31st. 1963	contract number 032-60-11 RDH
January 1st. 1964	- June 30th. 1965	contract number 030-64-1 TEEN
July 1st. 1965	- June 30th. 1966	contract number 069-65-7 TEEN.

Many Special Technical Reports have been published during these periods dealing with the results obtained from the experiments or the development of instrumentation. Ultimately, an extensive compilation of measuring techniques, measurements, analyzing techniques and theoretical studies has been published in the thesis of Spigt (ref. 1). In fact, this publication coincided with the rounding off of the measurements under natural convection. Since, the natural recirculation program has been complemented by a small series of experiments bearing a very special character: the effect of the response time of the heating element has been investigated.

The experiments have, then, been continued with forced circulation.

A short description of the experimental set-ups and the instrumentation equipment has been included. For a detailed description reference is made to the thesis of Spigt (ref. 1).

2. Description of the set-ups.

In the following a description will be given of the different loops and the power supply, which are in use in the research program aimed at studying the characteristics of a boiling water reactor.

(+) Manuscript received on April 18, 1968.

2.1. The pressurized boiling water loop.

In this loop it is possible to study the behaviour of a unit-cell of a boiling water reactor. A simplified drawing of the loop is given in Figure 8.

The test section consists of an electrically heated element placed inside a shroud, simulating a fuel element of a boiling water reactor with the right form and geometry. This test section is placed inside a cylindrical pressure vessel which is filled with water up to a level above the top of the test section.

When the element is heated the water between the element and the shroud starts to boil. The steam-water mixture flows upwards by natural convection through this annular passage, the riser. At the water surface the steam and water are separated. The waterflow returns through the annular passage between the shroud and pressure vessel wall, the downcomer, to the inlet of the riser. The steam flows to the condensor and the condensate is then returned to the downcomer passing a preheater.

The pressure vessel is made of stainless steel 316 and withstands a working pressure of 40 atmospheres. The cylindrical part has an inner diameter of 150 mm and a length of 3000 mm. The vessel is provided with the necessary connections for measuring equipment.

The water level is kept within certain limits by means of a water drum (stabilizer), which is connected to the pressure vessel.

A 3" diameter steam line leads to the condensor. The steam is condensed inside three coiled tubes by evaporating cooling water to the atmosphere. Condensor control is achieved by automatic control of the coolant water flow which is sprinkled on the condensor tubes.

The automatic control acts on the steam temperature in the pressure vessel and compares this with a reference value. The control is proportional, integrating and differentiating.

Parallel to the downcomer there is a subcooler, giving the possibility to subcool the returning water. Midway, the downcomer has been closed by a Teflon packing and the water is forced to return through the subcooler. The secondary circuit of the subcooler consists of four

spiralized tubes with vanes, through which demineralized water flows. For a closer control a preheater has been installed. By this sub-cooler about 250 kW heat can be removed at 230°C on the primary side.

The subcooler circuit can be extended with a stainless steel centrifugal pump and connecting tubes for carrying out forced circulation measurements. The pump is suitable for temperatures up to 250°C and pressures up to 40 atmospheres, and has a capacity of 35 m³/h. The material used for the heating elements is stainless steel hard soldered to the top and bottom electrodes. The electrodes are water cooled. An asbestos graphite packing with spring pressure at the bottom electrode allows for expansion of the element. Several types of heating elements have been tested, single rods as well as rod-clusters.

The shrouds separating the riser part from the downcomer part of the pressure vessel are made from stainless steel. Several types are available with different diameter.

2.1.1. Power supply.

In the laboratory a large power supply is available for heating the elements, which are fed by two transformers from the 10 kW mains. The transformers are cooled with oil by natural convection and are placed outside the laboratory. The rectifiers are placed inside the laboratory hall and are water-cooled.

The power can be excited with a frequency of about 8 cycles per second with an amplitude of about 20% of the mean value. In the whole voltage range a current can be given off of 14.400 Amperes, which means a maximum power of 860 kW.

The two rectifiers can be used independently or in series. Connected in series the available power is about 1.2 MW.

2.2. Atmospheric boiling loop.

The geometry of this loop is the same as that of the pressurized boiling loop. The element is heated by a 15 kW rectifier. In this loop

also, different types of heating elements and shrouds can be installed, while the inlet pressure drop can easily be changed. The steam is condensed in a small heat exchanger. A multimanometer is available for measuring pressure differences. This loop is used for visualization and study of instabilities and flow patterns.

3. Instrumentation.

In order to carry out the experimental program several instruments had to be developed, while the accuracy of existing methods had to be improved. Furthermore, use of special recording and analyzing apparatus had to be made. In the following a review is given of all the measuring, recording and analyzing equipment presently in use in the two-phase flow program.

3.1. Measuring equipment.

Void fraction measurements

Radioactive method

This method has been developed for measuring the void fraction at a fixed position at steady state conditions in the boiling water loop. A thulium-170 source of about 350 mC is placed inside the heating element. Opposite to the source the attenuated γ -quantum is measured by 4 scintillation detectors. The pulses of the detectors are mixed with a minimum of loss with pile-up of pulses by a special clipping technique, which is developed in the laboratory itself. The pulses are counted by a 10 Mc scaler, which is connected to a printer. The total dead time of the apparatus is 3.6μ sec. at count rates up to 60.000 counts/sec. The NaJ(Tl) crystal and the photomultiplier are water-cooled since the temperature in the loop may rise to 240°C .

Each photomultiplier is provided with an own high voltage supply. This gives the possibility to adjust the high voltage of each photomultiplier in that way that the amplifications of the tubes are the same. Then it is possible to discriminate over the thulium peak (84 keV) giving the best full to empty ratio. The amplification is automatically controlled by means of a spectrum stabilizer.

Impedance method

The system of measuring void fraction in non-steady conditions in electrical way as applied in this laboratory can be distinguished in techniques measuring the change in:

- 1) conductivity and
- 2) capacitance of a two-phase mixture with change in void fraction.

The measuring methods have been developed for an annulus with a single heating element. In both systems the heating element is used as one electrode while in the hull of the shroud four plates are placed around the element at given axial positions to act as sets of second electrodes.

The first method mentioned is working together with the radio-active method in the pressurized boiling loop; they show a very good agreement within $\pm 3\%$ void. In the second method very high frequencies must be applied. This has been developed on a small table loop.

It is stressed that both methods measure the void fraction without introducing any disturbance in the two-phase flow area.

Pressure gauges

In the laboratory fast gauges have been developed for dynamic measurements. The principle of the measuring method is that the change in capacitance, due to the displacement of a membrane with regard to a fixed and insulated electrode is measured by a capacitance displacement meter. The capacitance to be measured is placed in a LC resonance circuit.

Besides these especially developed pressure gauges, commercially pressure gauges of the inductive type are in use. The eigen frequencies of these gauges are lower than those of the home-made gauges.

Temperature, burn-out and elongation of the heating element

Temperature

For the accurate measurement of the steam and water temperatures and also of differential temperatures for the adjustment of the subcooling, chromel-alumel thermocouples, which are shielded and insulated by an inconel sheath, are being used.

The outer diameter of the sheath is 1 mm.

For non-steady state conditions thermocouples with thicknesses of 0.5 and 0.33 mm have been used. The signals of these couples have been recorded on a FM tape-recorder and on an ultra violet recorder.

Burn-out detector

To avoid burn-out of the heating element, a burn-out detector has been installed as a safety device. The upper and lower half of the heating element are placed in a Wheatstone bridge. Due to a temperature difference of these two parts, the bridge becomes out of balance, which is made visible on a trip galvanometer. When the needle contacts a preset limit switch, the power on the heating element is switched off.

A burn-out detector without a trip galvanometer can also be used for following the fluctuation in temperature in the heated rod, which occurs at some combinations of power, pressure and subcooling.

Elongation of the heating element

Since the heating element can expand downwards, this expansion is measured by an inductive type distance meter with a resolution of 2 microns. The indication of this instrument gives some information of the average temperature of the rod. In non-steady state conditions information can be obtained about the response of the rod to power or temperature fluctuations.

Heat generation measurement

The heat generated in the element and the preheaters is measured electrically in steady state conditions by means of precision voltage and current meters and of a light spot watt-meter.

For the measurement of the heat generated in the element in non-steady conditions use is made of commercially available so-called Hall generators. These instruments give a signal proportional with the product of voltage and current of the heating element. They have been calibrated at steady state conditions and analyzed for phase-shift and amplification up to 50 cps. The dynamic characteristics of these instruments are sufficient for the frequency range for which they will be applied. No corrections of measured signals are needed.

Flow measurements

Flowrate measurements are made by means of Δp measurements.

For steady state conditions use is made of a multimanometer and Barton differential pressure transducers. Differential pressure gauges of the inductive type with mV output are applied for dynamic measurement. The output is recorded on a FM tape-recorder and/or an ultra violet recorder. The multimanometer is used for calibration of the Barton differential pressure transducers and the inductive type pressure gauges. Also, the home-made pressure gauges are used.

3.2. Recording equipment.

Conventional recorders

For slow recording purposes use is made of commercial available continuously writing or printing recorders with temperature or mV scales. Most of them have a variable range and the possibility of zero-shift and zero-suppression.

UV-recorder and FM tape-recorder

The signals of flowrate, void fractions, water, steam and surface temperatures, pressures, burn-out detectors, elongation of the heating element and the Hall generator (power) can be continuously recorded at fast rates on a 16-channel ultra violet recorder, equipped with photographic paper.

For more detailed analysis purposes the signals can also be recorded on a 14-channel Frequency Modulated Magnetic tape system at 6 different speeds.

Automatic read-out equipment for steady state conditions

This equipment consists of a 20 point scanner, digital voltmeter, encoder and printer. The speed of this equipment is 5 numbers of 12 decimals in 2 seconds. It is in use for automatically printing out of the data in decimal form in steady state conditions.

Data logger for non-steady state conditions

This data logger consists of:

- a) a 500 channel scanner
- b) an analog to digital converter with a conversion speed of max. 1000/sec.
- c) a pre-amplifier which has an adjustable range setting of 10 to 10.000 mV.
- d) a puncher with a speed of 110 characters/sec.

Any numbers of scanning points from 1 to 500 and any sequence of these points can be programmed by means of pushbuttons and plugs. Also, the sampling rate and the sampling time can be adjusted separately. These are kept constant between points in one cyclus as well as between points in successive cycli. This is especially important in a digitizing process for noise analysis in terms of auto- and cross-correlations and power curves. This equipment has been used in connection with the magnetic tape system or directly in line with the process.

High speed camera

For studying the formation and growth of bubbles on a heated surface and flow types occurring in a two-phase mixture a high speed film camera, Beckman & Whitley, Dynafax - 316, has been purchased.

A continuously adjustable speed is possible in a range of 200 - 26.000 frames per second. Studies with this apparatus are made about instabilities in the atmospheric glass boiling loop.

Printer

For the radioactive method use is made of a decimal printer, which receives the coded information from a 10 Mc counter. The printer can also be connected to 4 or 5 digits Digital Voltmeters, which are available in the laboratory and to the automatic read-out equipment.

3.3. Analyzing equipment.

Analogue computer

An analogue computer, type PACE, present in the laboratory is being used for the studies of the mathematical description of the behaviour of a boiling water loop and reactor. This machine will also be used in combination with the boiling loop. Signals from the loop will be fed into the analogue machine while this is controlling the power supply of the loop. The machine will then simulate reactor neutronics. In this way it is possible to study the feedback behaviour of a boiling water reactor. The analogue computer is a PACE R-231 equipped with 120 amplifiers, 18 multipliers and 6 function generators, a digital voltmeter and an automatic print out device. Furthermore, a plotter is available and besides an 8-channel Sanborn recorder.

Digital computer

On the IBM-1620 computer of this University computations have been carried out regarding the characteristics in steady state conditions of the boiling loop.

At present an Electrologica X-8 computer is available at the University

which is used for digital analysis of the measurements as well as for more extensive calculations.

The programs are written in Algol.

Most programs are related to studies of the behaviour of a natural circulation boiling loop in steady and non-steady states and to the analysis of experimental results.

Furthermore a program has been written calculating the transfer function from two noisy but correlated signals by computing auto- and crosscorrelations and auto- and cross spectra.

Transfer function analyzer

Besides by digital means, transfer functions can also be determined in an analogue way, giving the results more directly. Difficulties arise from the presence of noise on the output signals from the experimental loop sometimes in a ratio of 10 to 20 over 1. This can be overcome by using an apparatus which performs a Fourier analysis of the output response. In the Laboratory, a Transfer Function Analyzer type Boonshaft works on this principle. With this equipment the analysis can be carried out in terms of transfer functions of sinusoidally excited response signals, whereas it is possible to measure transfer functions from point to point in a system directly. The point to point frequency response is desirable when the frequency response must be measured between two points A and B in a system in the case that the system cannot be excited sinusoidally in these points, but has to be excited at another point.

A complementary part makes transfer function calculations possible between two noise signals without the need of using the internal excitation signal and enables besides to apply a transient power input.

Noise correlator

The noise correlator ISAC (Instrument for Statistical Analog Computation), present in the laboratory, is a special purpose analogue machine and can be characterized as follows:

- a) it records three electrical signals simultaneously on a magnetic tape in a frequency range of 0-200 cps.
- b) it calculates of the recorded signals:
 1. the auto- and crosscorrelations
 2. the power density and amplitude density curves
 3. the first order amplitude distribution function

- c) it calculates entirely automatically and the results are presented graphically on a X-Y-recorder.

Measurements.

In the following a review will be given of the experiments carried out in the two-phase flow research program. The description will not be restricted to the status at the time of expiration of the contract but will also include a number of experiments carried out after this date.

4.1. Measurements with natural circulation.

Most of the results of the measurements have been reported in topical reports and an ample description of the measurements is given in the thesis of Spigt (ref. 1). This thesis covered all of the results obtained in the first part of the program dealing with natural circulation.

The conclusions of this report are cited here and some figures have been added to support the statements.

The results of an experimental and theoretical study have been reported on the steady state and stability characteristics of a naturally circulating boiler. In general it can be said that there is a lack of systematic data on the onset of hydraulic flow oscillations and on the stability characteristics of a two-phase flow in dependence of the operating conditions. Furthermore, there is a need for more detailed information, theoretical as well as experimental, in order to obtain a better characterization of the various types of flow oscillations. The work described gives a contribution towards a better understanding of the two-phase flow stability characteristics.

One of the most important variables determining the heat transfer and fluid flow characteristics of a boiling channel is the void fraction. Therefore, much work has been devoted to the development of a new technique for void fraction measurement, i.e. the impedance void fraction method. As appears from the results, this measuring method is entirely suitable for void measurement under steady state and transient condi-

tions. The method is simple and inexpensive in comparison with the γ -ray attenuation technique. Similar experiences have been reported in (C2) and (O1). Although the impedance method is particularly suited to void fraction measurements in transient conditions, the γ -ray attenuation technique may be better suited for void distribution measurements. (Fig. 1).

In the experimental program, use has been made of the characteristics of the noise, expressed in autocorrelations, crosscorrelations, spectral power densities and cross-power densities in determining the onset and character of flow oscillations and the stability characteristics of a steady state in terms of transfer functions. The application and the effectivity of noise analysis in obtaining information on the dynamic behaviour of a two-phase system has been demonstrated. The crosscorrelation technique has been found to be a powerful technique for eliminating the effects of external noise. The technique using a harmonically oscillating input yields accurate results, but the required measuring time is long. Some improvement may be gained by application of a multi-frequency signal method. The application of the analysis of the inherent noise asks for further development and evaluation work. (Fig. 2).

Results were given of measurements determining the steady-state performance characteristics of the boiling channel with natural circulation. An attempt was made to plot the results in terms of non-dimensional quantities for the heat load, subcooling, pressure and for the dependent quantities. Although this was not successful, it would be interesting to continue the analysis in this way and to include experimental results from other sources, especially from those carried out with other liquids.

An analysis of the experimental results was made in terms of the Slip Ratio, S , and the Two-Phase Friction Multiplier, R . It was shown that the slipratio is a ratio of weighted average phase velocities and therefore dependent on the distribution of the void fraction across the channel. Furthermore, it has been shown that, in deriving two-phase friction losses from pressure measurements along a boiler, accurate results can only be obtained when the influence of the cross-sectional distributions

is understood.⁽³⁾ The void fraction data were plotted in the "weighted mean velocity-average volumetric flux density" plane, proposed in (Z1). From this plot it may be deduced that flat profiles for the velocity or concentration distributions are present under the operating conditions reported. (Fig. 4).

Although the work reported in (B14), (T2), (V4) and (Z1) contributed a great deal towards the knowledge of the characteristics of a two-phase mixture, more development is needed, particularly as regards the recognition of flow regimes and the theoretical and experimental prediction of concentration and velocity distributions over the cross-section of the flow channel. This is a prerequisite to any further analysis of the presented steady-state data. The presently available experimental correlations for S and R are not altogether satisfactory in this respect.

During operation it was possible to distinguish between three types of flow oscillations with frequencies of roughly .03, 1 and 15 c.p.s. By adopting a criterion for defining the onset of the 1 c.p.s. hydraulic oscillations, the influence has been systematically measured of the system pressure, subcooling and hydraulic diameter on the instability threshold channel power. At high system pressures, there was a gradual increase in amplitude of the flow oscillations with increasing channel power, in contrast with low system pressures, at which the flow oscillations tend to start more spontaneously. At low subcooling rates, increased subcooling precipitates, and at high subcooling rates this postpones the onset of severe hydraulic oscillations. This effect is more pronounced at high system pressures and for test sections with large hydraulic diameters. Any increase in hydraulic diameter postpones the onset of hydraulic oscillations to higher channel powers. Recordings of the relevant physical quantities revealed that during hydraulic oscillations the void fraction near the inlet and outlet of the coolant channel were roughly 180° out of phase. The same was true for the void fraction and the mass flow rate at the inlet. (Figs 5 and 6).

The influence of the operating conditions on the stability of a steady-state, when expressed in transfer functions, was similar to that on

the instability threshold channel power. It was also found that, as regards the stability characteristics, the influence of increased subcooling at low subcooling rates is opposite to that at high subcooling rates. From the transfer function measurements it could be concluded that the two-phase flow process may be regarded as a linear process for small disturbances from the steady state, even at high channel powers.

Characteristic of all measured transfer functions was the appearance of a sharp resonance peak when the instability threshold was approached (fig. 7). The resonance peak is characteristic of a naturally circulating system and is caused by a strong intercoupling between the steam void and the inlet mass flow. The flow oscillations appear owing to the fact that this intercoupling becomes unstable, and not to the fact that the flow is responding to a present boiling instability or flow-pattern instability. The intercoupling effects are strongly influenced by the boundary conditions. It is, therefore, clear that in an analysis of hydrodynamic instability, not only the region of the two-phase flow, but the entire system, including the downcomer, and, if necessary, the pump characteristics have to be taken into account. Furthermore, any study of the flow oscillations must start from equations incorporating dynamic effects. A stability analysis based on steady-state characteristics as, for instance, proposed in (L3), is only of limited value.

Burn-out channel powers and heat fluxes have been presented for various values of system pressures and subcoolings. Nearly all burn-outs were obtained under unstable flow conditions. The results confirm the belief that hydraulic instability plays an important role in burn-out. It would be interesting to repeat some of the experiments under conditions of forced circulation and with a heating element having a different time constant. Besides, it might be of interest to investigate the effect of inlet throttling on the burn-out heat flux, even under stable flow conditions.

A set of basic equations has been derived describing the performance characteristics in steady-state and transient conditions of a boiling system. These equations have been integrated over the cross-section

of the coolant channel. Owing to this integration, it was shown that correlations have to be introduced which account for distributional effects. Special attention has been paid to the formulation of the boundary conditions and the introduction of pressure effects. As was shown in the analysis of the experimental results, the two-phase flow process may be regarded as a linear process for small disturbances from the steady state. Therefore, the derived equations were linearized. By considering an "open"-loop, two stability criteria were defined for detecting the onset of flow oscillations. These criteria are defined by means of the transfer functions for the "open"-loop from an imposed variation in saturation temperature at the inlet to the resulting variation in saturation temperature and mass flow rate at the outlet of the downcomer. It might be concluded that an instability determined by the latter transfer function is related to a forced convection boiler incorporating a pump with steep headflow characteristics in which resonance conditions may appear within the boiling channel. The first mentioned transfer function is related to a natural circulation boiler.

Preliminary results of the steady state performance and "open"- and "closed"-loop characteristics have been reported. The steady state performance characteristics as well as the instability threshold channel powers predicted theoretically were in good agreement with the measured data. Furthermore, it was shown that also in the very low and high frequency region, flow oscillations may develop. The experimentally determined character of the 1 c.p.s. flow oscillations was similar to that predicted theoretically. The 1 c.p.s. flow oscillation resembles more or less a standing wave, i.e. it represents approximately a half wavelength oscillation in the velocity distribution.

It will be necessary to extend the theoretical description with an energy equation for the heating element. Only then will it be possible to compare the theoretically and experimentally obtained closed-loop characteristics in detail. Moreover, further analysis work is necessary regarding the phenomena governing the onset and character of the hydraulic instabilities and concerning the choice of which parameters are of less significance and may hence be safely disregarded. In a further

study attention must also be given, particularly in the low frequency range, to the pressure-drop characteristics of a boiling channel and to the influence of the condensor and subcooler characteristics on the stability.

Since then, a small series of additional experiments with natural circulation has been carried out in order to investigate the influence of the response characteristics of the heating element on the stability as well as on the burn-out conditions. Two types of heating elements have been used. The results have been presented at the Symposium On Two-Phase Flow Dynamics, held in Eindhoven in September 1967 (ref. 2). Because the emphasis of these measurements has been put upon the comparison with the results obtained from a mathematical approach these results will be reviewed briefly in chapter 5.

4.2. Measurements with forced circulation

The boiling loop has been provided with a pump in the downcomer in the way as indicated in fig. 8. No other changes relative to the natural circulation set-up have been introduced. A preliminary series of measurements has been carried out in order to study the steady state and dynamic behaviour of the boiling system with forced circulation. The results have been published in a report presented at the Symposium held in Eindhoven September 1967 (ref. 2) and will be repeated here.

During the measurements under forced circulation, the impedance gauges for measuring the void fraction did not work quite satisfactorily. For this reason only the pressures along the channel axis have been given as a function of the distance from the channel inlet and have been compared to the values obtained from measurements under natural convection (see fig. 9). The numbers plotted represent the readings from the manometer which still have to be corrected for the ρgh terms due to the different lengths of the pressure tappings.

The system pressures at which the forced circulation experiments have been carried out were chosen 2, 15 and 31 kg/cm² corresponding to

saturation temperatures of 120, 200 and 234°C respectively. The values of the inlet flowrate were chosen such as to be able to interpolate the results to corresponding conditions under natural circulation. The subcooling has been kept as low as possible but due to the limited power of the trimheater placed in the waterline at the bottom of the subcooler, the subcooling increased when low values of flowrate were established.

The close agreement between the pressure curves of natural and forced circulation experiments suggests the conclusion that the difference in void fraction must be very small supposing that the different flow profile has only a little effect.

Non-steady state

It appeared to be possible to generate spontaneous oscillations only at a saturation temperature of 120°C. For all conditions the experiments were continued until burn-out occurred i.e. until the burn-out detector switched off the channel power. The maximum inlet velocity at which the burn-out point could be reached at the saturation temperatures of 200°C and 234°C was 1.5 m/sec. At higher velocities the capacity of the steam condensor was the limiting factor for increasing the power. This means that it could not be investigated whether at higher pressures unstable conditions should be encountered at higher values of the inlet velocity.

The lowest flowrate at which instabilities occurred at a saturation temperature of 120°C was very close to zero. The valve in the pumpline was fully closed. The pressure difference across the inlet was not really readable from the multimanometer. This implies except an almost zero flowrate, only present owing to internal leakage of the butterfly valve, also a very high inlet throttling. Notwithstanding this condition, the flowrate and void fraction started to oscillate at about 60 kW (see fig. 10a). The oscillations increased in amplitude when raising the power up to 100 kW. However, when raising the power by again 10 kW the instabilities disappeared abruptly and the ampli-

tudes dropped down to the normal noise level. The burn-out occurred at 150 kW at stable flow conditions.

At a flowrate of 1.5 m/sec the threshold of instabilities was at 325 kW. In this case increasing power caused increasing amplitudes of the oscillations over the whole range until burn-out occurred at 340 kW (fig. 10b). The difference with the previous condition was except the different flowrate the much lower inlet throttling of the boiling channel resulting in a less stiff connection between boiling channel and downcomer.

The frequency of the oscillations was at nearly zero flowrate .9 Hz, in agreement with the frequency measured under similar conditions with natural circulation. When considering the total length of the downcomer being as much as 3 times as long as under natural circulation one must conclude that the frequency is not a function of the downcomer length.

At a flowrate of 1.5 m/sec the frequency decreased to .6 Hz due to a higher subcooling. This subcooling has been kept to a minimum during the measurements by means of a trimheater (see fig. 8) but at higher channel powers the limited capacity of the condensor caused subcooling of the condensed liquid which could not be fully compensated by the trimheater. The subcooling at the inlet of the boiling channel amounted to about 11.5°C.

Considering the U.V. recordings that have been made of the Δp_{inlet} and of the void signals, the last signals show a largest amplitude at the height of the boiling boundaries as indicated in the figs 11 and 12. The same show the void signals recorded under natural convection (fig. 5) taken from ref. 1.

The void signals recorded at a power of 335 kW and given in fig. 12 indicate a phase shift between the signals in that way that the signal of each void gauge has a phaselag compared to the signals of void gauges situated at lower axial positions (lower numbers correspond to higher positions).

Transfer function measurements

In order to measure transfer functions use has been made of a special purpose analogue computer, called "Transient Frequency Response Analyzer" made by Boonshaft.

An oscillator generates a sine wave which represents the input signal as applied for these experiments to modulate the power. A Fourier analysis of two selected output signals provides the transfer function. Transfer function measurements under forced circulation have been made at conditions of 200°C saturation temperature and inlet flowrates of .2, .9, 1.2 and 1.5 m/sec from the modulating power signal to the signals of Δp_{inlet} and various voids.

The amplitude of the power signal amounted to ± 10 percent of its mean value.

At a flowrate of .9 m/sec the transfer functions from power to Δp_{inlet} taken at four different power levels as given in fig. 13 show peaks at about .9 Hz. However, the amplification is not continuously increasing with the power level. To check this behaviour this transfer function has been determined at a constant frequency of .9 Hz and different power levels (fig. 14).

The curve shows indeed a maximum amplification at a mean power of 140-145 kW. At increasing the power beyond this value the amplification drops down. This is in close correspondence to the influence of the power on the instabilities detected at 120°C and nearly zero flowrate. However, at 200°C this did not lead to spontaneous oscillations. At steady state conditions and equal flowrate burn-out occurred at 290 kW. Some transfer functions measured under similar conditions but with natural circulation are given in fig. 13 and show much steeper and higher peaks, the one corresponding to 145 kW being higher than the one corresponding to 113 kW. In this case 145 kW was close to burn-out.

The curves of the argument are flatter than those under natural convection which support the trend of the moduli.

The frequencies compare very well, being in agreement with those of fig. 11.

In order to shorten the time needed for the experiments a number of

signals from six usable void gauges have been recorded on a magnetic tape, together with the signal from the power. Afterwards, these signals have been analyzed, making use of the T.F.R.A. apparatus, just like during the direct measurements. The amplitudes of the signals of the three upper void gauges were too small to get reproducible values. The results are given in fig. 15. The amplitude of the void signals in response to the modulating power signal is continuously decreasing with the frequency interrupted by a small peak at .9 Hz. This behaviour indicates a strongly damped system as can be expected. For comparison fig. 16 is added showing a similar figure measured under natural circulation. However, the power is different. The peaks of the curves are more pronounced.

The arguments in fig. 15 show an increasing phaselag with respect to the modulating power signal with increasing distance from the bottom of the shroud. This is due to a superposition of the voids of the lower positions, moving upwards, to the void generated at higher positions. The curves of the argument in fig. 16 are steeper (notice the different scale of the angle), corresponding to the higher peaks of the modulus.

5. Theoretical studies.

5.1. Linearized model

The main effort has been focussed on the development of a linearized, distributed parameter study of the hydraulic behaviour of the system for a description of which reference is made to (ref. 4).

Introduction of changes

The following changes relative to the model explained in (ref. 4), have been introduced into the model:

- a) In the boiling section the two energy equations, one for the water phase and one for the steam phase, have been lumped together.

- b) The model has been made applicable to calculations with forced circulation by incorporating a pump characteristic.
- c) The model has been extended by the incorporation of the response characteristics of the heating element.

5.1.1.a. Summation of the energy equations

Originally (ref. 1) the energy equation in the boiling region has been split up into two parts similar to the way in which it has been done for the subcooled boiling region i.e. the energy input term of the energy equation for the water phase reads $(1-\kappa)Q'$ for the steady state conditions and the one for the steam phase reads Q' . In the region of subcooled boiling this κ represents the heat distribution parameter as for instance suggested by Bowring (ref. 3) and in the bulk boiling region this κ , which could better be replaced by another symbol here, effects, if larger than one, the amount of superheat of the liquid. Because of the presence of κ in the right members of the equations it does not solely influence the superheat. It is not possible to impose a well-defined amount of superheat. Therefore, the energy equations have been summed together which raises the need of another, fourth equation in order to define the relation between the fluid temperature and the steam temperature. In the literature most of the authors assume an equality between both temperatures but in this model the possibility has been accepted to adjust a certain amount of superheat.

5.1.1.b. Incorporation of a pump

The general form of the pump characteristic was assumed to be $\Delta p = f(v)$ and more specifically $\Delta p = c_1 v^2 + c_2 v + c_3$ where Δp represents the pressure increase at the inlet of the channel, generated by the pump, v the inlet velocity of the channel and c_1 , c_2 and c_3 constants dependent upon the pump considered.

For the steady state case this pressure increase has been added to the momentum equation of the boundary conditions, imposed by the downcomer of the system.

In the non-steady state system it appears to be sufficient to replace in the momentum equation the constant κ_{ci} , which determines the inlet friction loss by

$$\kappa_{ci} = \frac{\partial f(v)}{\partial v}$$

5.1.1.c. Incorporation of the dynamic characteristics of the heating element

The model has been refined further by incorporating the heat transfer characteristics of the heating element. The general equation governing the process of heat transfer from the power supplied to the heating element to the power transferred to the fluid is given by:

$$\frac{Q}{A} + \frac{\lambda_m}{r} \cdot \frac{\partial}{\partial r} \left(r \frac{\partial T}{\partial r} \right) = \rho_m c_m \frac{\partial T}{\partial t}$$

where:

Q	represents the heat supplied to the heating element per unit length	
A	the cross section of the element	
r	the radius of the element	
T	the temperature of the heater wall	
λ_m	the thermal conductivity	} of the tube material
c_m	the specific heat	
ρ_m	the specific weight	

Conduction of heat in axial direction has been neglected.

Introducing harmonic disturbances and applying the transformation

$u = z\sqrt{\frac{-i}{\sigma}}$ yields the general solution:

$$T_i = B_1 J_0(z\sqrt{\frac{-i}{\sigma}}) + B_2 Y_0(z\sqrt{\frac{-i}{\sigma}}) + \frac{Q_i}{\rho_m c_m A \omega_i} \quad (1)$$

where:

J and Y represent Bessel functions

B_1 and B_2 constants to be solved from the boundary conditions

$$z = \frac{r}{r_o} = \frac{\text{radius of the rod}}{\text{outer radius of the rod}}$$

$$\sigma = \frac{\lambda_m}{\rho_m c_m \omega r_o^2}$$

ω = the circle frequency

subscript i designates the non-steady conditions.

The surface temperature T_{wi} can be found by putting $z=1$, so

$$T_{wi} = (T_i)_{z=1} \quad (2)$$

Two additional equations play a role, namely:

1. the heat flux passing the tube wall in radial direction Q_{ai} is given by:

$$\frac{Q_{ai}}{2\pi r_o} = - \lambda_m \left(\frac{\partial T_i}{\partial r} \right)_{r=r_o} \quad \text{or}$$

$$\frac{Q_{ai}}{\lambda_m} = - 2 \pi \left(\frac{\partial T_i}{\partial z} \right)_{z=1} \quad (3)$$

2. the heat transferred to the fluid is governed by:

$$Q_{ai} = 2\pi r_o h (T_{wi} - T_{fi}) \text{ in which}$$

T_{fi} represents the temperature of the fluid (assumption of a flat temperature profile)

$$\text{and } h = n \cdot (T_{wo} - T_{fo})^{n-1} \cdot h_n$$

with h_n being the steady state heat transfer coefficient.

The boundary conditions given by the heating element under consideration determine the values of B_1 and B_2 in equation (1).

Solid bar

For a solid bar the boundary condition is:

$$\left(\frac{\partial T_i}{\partial z}\right) = 0 \text{ at } z=0, \text{ which gives } B_2 = 0$$

The unknown parameters remaining in the equations 2, 3 and 4 are T_{wi} and B_1 . Elimination of these parameters and substituting $A = \pi r_o^2$ gives:

$$\frac{Q_{ai}}{Q_i} = \frac{\frac{1}{i} - \frac{\lambda_m \pi T_{fi}}{\sigma Q_i}}{\frac{\pi}{8\sigma} - \frac{1}{2\sqrt{-i}\sigma} \cdot \frac{J_0(\sqrt{\frac{-i}{\sigma}})}{J_1(\sqrt{\frac{-i}{\sigma}})}} \quad \text{where } \delta = \frac{2\pi r_o h}{\lambda_m} \quad (5)$$

From this equation two time constants can be derived, namely:

$$\tau_1 = \frac{\rho_m c_m \cdot 2\pi r_o^2}{\lambda_m} \quad \text{and} \quad \tau_2 = \frac{\rho_m c_m r_o \pi}{h}$$

The first one is only a function of the dimensions and the material properties of the element and determines the radial

heat transport, whereas the second one mainly depends on the heat transfer coefficient and consequently determines the heat transport from the heated surface to the fluid.

Tubular element

For this type of element the boundary condition reads:

$$\frac{\partial T_i}{\partial z} = 0 \quad \text{for } z = \frac{r_i}{r_o} \quad (6)$$

In this case it appears to be impossible to estimate easily the value of B_2 . The three unknown parameters B_1 , B_2 and T_{wi} have now to be solved from equations 2, 3, 4 and 6. The solution is somewhat complicated compared to the one of the solid bar; therefore for a detailed derivation reference is made to (ref. 4).

Ultimately the following transfer function results:

$$\frac{Q_{ai}}{Q_i} = \frac{1 - \frac{\lambda_m \pi}{\sigma} \cdot \frac{T_{fi}}{Q_i}}{\frac{(1-\eta^2)\pi}{\delta \sigma} - \frac{(1-\eta^2)}{2\sqrt{-i\sigma}} \cdot z} \quad \text{where} \quad (7)$$

$$\eta = \frac{r_i}{r_o} \quad \text{and} \quad z = \frac{J_0\left(\sqrt{\frac{-i}{\sigma}}\right)Y_1\left(\eta\sqrt{\frac{-i}{\sigma}}\right) - J_1\left(\eta\sqrt{\frac{-i}{\sigma}}\right)Y_0\left(\sqrt{\frac{-i}{\sigma}}\right)}{J_1\left(\sqrt{\frac{-i}{\sigma}}\right)Y_1\left(\eta\sqrt{\frac{-i}{\sigma}}\right) - J_1\left(\eta\sqrt{\frac{-i}{\sigma}}\right)Y_1\left(\sqrt{\frac{-i}{\sigma}}\right)}$$

The time constants appearing from equation 7 are:

$$\tau_3 = \tau_1(1-\eta^2)^2 \quad \text{and} \quad \tau_4 = \tau_2(1-\eta^2)$$

The mathematical treatment of equations 5 and 7 in addition to the linearized model of the hydraulic system is very time consuming. Therefore an attempt was made to obtain sufficiently accurate results by approximating the exact solution by means of a series expansion.

When the heat transfer coefficient h is considered to be infinite and realizing that this implies that $T_{wi} = T_{fi}$ equation 5, valid for a solid bar, can be simplified to:

$$\left(\frac{Q_{ai}}{Q_i}\right)_{T_{wi}=0} = \frac{2}{\sqrt{-i}} \cdot \frac{J_1(\sqrt{-i})}{J_0(\sqrt{-i})} \quad .$$

The well-known series expansion for this equation reads:

$$\left(\frac{Q_{ai}}{Q_i}\right)_{T_{wi}=0} = \sum_{n=1}^{\infty} \frac{D_n}{1+i\omega \Theta_n} \quad \text{where}$$

$$\Theta_n = \frac{1}{a \cdot \beta_n^2} \quad \text{with} \quad a = \frac{\lambda_m}{\rho_m c_m} \quad \text{and} \quad \beta_n = \frac{z}{r_o} \sqrt{\frac{-i}{\sigma}}$$

$$D_n = \frac{4}{(r_o \beta_n)^2}$$

$$r_o \beta_n \text{ are the roots of } J_0(r_o \beta) = 0$$

The complementary transfer function can similarly be written as:

$$\left(\frac{Q_{ai}}{T_{wi}}\right)_{Q_i=0} = 2\pi \lambda_m \sqrt{\frac{-i}{\sigma}} \cdot \frac{J_1\left(\sqrt{\frac{-i}{\sigma}}\right)}{J_0\left(\sqrt{\frac{-i}{\sigma}}\right)}$$

Series expansion gives $\left(\frac{Q_{ai}}{T_{fi}}\right)_{Q_i=0} = - \sum_{n=1}^{\infty} \frac{B_n i \omega}{1 + \theta_n i \omega}$

with $B_n = 4\pi \lambda_m \theta_n$

The original exact equation (5) is recovered when making use of the equation $Q_{ai} = h \cdot 2\pi r_o (T_{wi} - T_{fi})$ with a finite heat transfer coefficient.

A first order approximation is obtained by putting:

$$\sum_{n=1}^{\infty} \frac{D_n}{1 + \theta_n i \omega} \approx \frac{\sum D_n}{1 + \sum \theta_n i \omega} = \frac{1}{1 + \sum \theta_n i \omega} \quad (8)$$

assuming that $\sum_{n=1}^{\infty} D_n = 1$

For a solid bar $\tau_s = \sum_{n=1}^{\infty} \theta_n = \frac{r_o^2}{4a}$

Calculations with this expression indicate an important difference with the exact solution concerning the amplitude as well as the phaseshift. Also the application of some more time constants in eq. 8 does not give the requested agreement.

The best fit appears to be obtained when considering the following expression, still based upon equation (8):

$$\left(\frac{Q_{ai}}{Q_i}\right)_{T_{fi}=0} = \frac{1}{\sqrt{1 + \tau_s i \omega}}$$

The limitation of this equation owing to the assumption that $h = \infty$ can be remedied by adding an extra term to the nominator as follows:

$$\left(\frac{Q_{ai}}{Q_i}\right)_{T_{fi}=0} = \frac{1}{\sqrt{1 + \tau_s i \omega} + \frac{\lambda_m r_o i \omega}{2ha}} \quad (9)$$

A similar derivation for the complementary transfer function reads:

$$\left(\frac{Q_{ai}}{T_{fi}}\right)_{Q_i=0} = \frac{-i\pi \lambda_m r_o^2 \omega/a}{\sqrt{1 + i\omega \tau_s} + i \frac{\lambda_m}{2h} \cdot \frac{r_o \omega}{a}} \quad (10)$$

These equations are simpler than equation (5) and show nevertheless an almost perfect agreement (fig. 18) with this equation 5.

For a tubular element similar approximations can be applied which ultimately results in:

$$\left(\frac{Q_{ai}}{Q_i}\right)_{T_{fi}=0} = \frac{1}{\sqrt{1 + \tau_t i \omega} + \frac{\lambda_m r_i i \omega}{2ha} \cdot \frac{(1 - \eta^2)}{\eta}} \quad (11)$$

and

$$\left(\frac{Q_{ai}}{T_{fi}}\right)_{Q_i=0} = \frac{-\pi \lambda_m \frac{r_o^2}{a} i \omega (1 - \eta^2)}{\sqrt{1 + \tau_t i \omega} + \frac{\lambda_m r_o i \omega}{2ha} (1 - \eta^2)} \quad (12)$$

where

$$\tau_t = \frac{r_o^2}{4a} (1 - \eta^2)^2 \quad \text{see fig. (19)}$$

Equations 9, 10, 11 and 12 have been incorporated in the linearized description of the boiling water loop.

Results of the calculations and comparison with experiments.

Preliminary calculations have been carried out to investigate the influence of the behaviour of the heating element on the hydraulic characteristics. The conditions that have been chosen were a saturation temperature of 200°C and zero subcooling. The results indicate that nor a solid bar nor a tubular element does have any effect on the threshold or the frequency of instabilities, as compared to the values obtained from the model where the characteristics of the heating element have been left out.

However, as is to be expected, the transfer functions are different (see fig. 20), where the transfer function from power to inlet velocity has been plotted. At conditions of a saturation temperature of 200°C , zero inlet subcooling and channel power 80 kW, the amplitude is lower with increasing mass of the element. The extra phaseshift introduced by the heating element appears to be less dependent upon the mass.

These results agree very well with those obtained from experiments. Normally the heating element used is a tubular one having a wall-thickness of 3 mm and an outer diameter of 33.8 mm. For the aim of comparison a solid bar has been applied with the same outer diameter.

The power generated instantaneously in the heating element is on the one hand, going into the fluid but is, on the other hand, used for increasing the temperature of the heating element itself. The power that easily can be measured is the instantaneous total power, but the net instantaneous power which is supplied to the fluid and which should be the correct power for correlating the transfer functions cannot be measured directly, nor can the power dissipated in the heating element. A measure for this latter power can be found in the elongation of the heating element. This elongation has been measured during the experiments by means of an

impedance displacement gauge. Fig. 20 shows the transfer function of the input power to the elongation of the element. The transfer function is measured for the solid bar at three system pressures. The operating pressure appears to have only a small effect on the transfer function. As can be expected from the magnitude of the time constants for power transmission to the coolant, the response to the power modulations is rapidly decreasing with increasing frequency in the frequency range studied. Fig. 21 shows the transfer function of the input power to the elongation of the element for the two types of rods as measured under forced circulation. The elongation is correlated with the mean temperature of the element. The solid bar has a higher mean temperature so that the quasi steady state gain of the solid bar is appreciable higher than by the tubular element. The fall off of the solid bar transfer function is much stronger than that of the tubular element. At .2 Hz the attenuation of the solid bar dominates. The phase-shift of the solid bar is much stronger which corresponds with the higher time constant of the solid bar. Fig. 22 shows the transfer function from power to flowrate for two different heating elements and for two different powers. It appears that already at a frequency of .1 Hz the two transfer functions differ by a constant gain. The gain factor is given by the ratio of the two time constants:

$$T_2/T_4 = \frac{1}{1-\eta^2} = \frac{r_2^2}{r_2^2 - r_1^2} = 2.86,$$

which means that the transfer function $(\frac{Q_{ai}}{Q_i})_{T_{fi}=0}$ of the heating element, if considered as a first order system with one time constant, has already reached the $\omega = \infty$ asymptote at a relatively low frequency. The

slope of this asymptote, being equal for both types of elements, results in a constant ratio of the transfer functions mentioned.

When looking at equations 9 and 10 the same constant ratio of the two transfer functions can be obtained taking the heat transfer coefficient h infinite. This tends to conclude that in reality this parameter h in a boiling channel is very large, that is to say $> 2 \cdot 10^4$.

The difference in phaseshift is for both types of elements negligible small at frequencies larger than .2 Hz emphasizing the behaviour like a first order system.

Also experiments have shown that the type of heating element does not have any effect on the threshold of instabilities nor on the burn out power. The measuring conditions were 120, 200 and 234°C saturation temperature with zero subcooling and 200°C with 11° subcooling at the inlet.

5.1.2. Improvements to be introduced into the linearized model in the near future.

1. It has commonly been assumed that the influence of subcooling on the stability of a boiling system is ambiguous. Low subcooling tends to destabilize the system and high subcooling to stabilize it. One of the lacks of the present linearized model is, that it does not display this effect. This has led to a further detailed study of the formulation of the basic equations. It appeared that the splitting up of the energy equation in the region of subcooled boiling did not correspond to the theory of Bowring as published in (3). Bowring states that the heat supplied to the fluid in the region of subcooled boiling is at the one hand going to increase the fluid temperature and at the other hand to generate vapour. In the present model, however, this latter part of the heat is not exclusively used to

form vapour but also to heat the mass of the water that is going to be transformed into steam up to the local saturation temperature, according to the following equations.

Energy equation for the liquid phase:

$$\frac{\partial}{\partial \zeta} (1-\alpha) (\rho_f v_f c T_f + p v_f) + \frac{\partial}{\partial t} (1-\alpha) \rho_f c T_f = (1-\kappa) Q$$

and for the steam phase:

$$\frac{\partial}{\partial \zeta} \alpha (\rho_s \gamma v_f (c T_s + r_s) + p \gamma v_f) + \frac{\partial}{\partial t} \alpha \rho_s (c T_s + r_s) = \kappa Q$$

Bringing the equations into closer agreement to the equations as suggested by Bowring implies removing of the $c T_s$ -terms from the vapour part of the energy equation and adding them to the liquid part.

This results in:

for the liquid phase:

$$\begin{aligned} \frac{\partial}{\partial \zeta} (1-\alpha) (\rho_f v_f c T_w + p v_f) + \frac{\partial}{\partial \zeta} \alpha \rho_s \gamma v_f c T_s + \frac{\partial}{\partial t} (1-\alpha) \rho_f c T_f \\ + \frac{\partial}{\partial t} \alpha \rho_s c T_s = (1-\kappa) Q. \end{aligned}$$

and for the steam phase:

$$\frac{\partial}{\partial \zeta} \alpha (\rho_s \gamma v_f r_s + p \gamma v_f) + \frac{\partial}{\partial t} \alpha \rho_s r_s = \kappa Q.$$

This change, which is of a rather essential nature, is being incorporated into the model.

2. Returning to the modification of adapting the model to forced circulation a separate iteration process has to be developed to enable adjusting a chosen inlet velocity. This can be done by effecting the value of the restriction at the inlet i.e. k_{ci} . This work is still to be done.

5.2. Brief review of the "Basic Principles" model.

The aim of this study has been to provide a fundamental theoretical approach to an understanding of the hydraulic behaviour of a two phase flow under steady state and transient conditions.

Especially the following phenomena are essential for this model:

1. The generation of bubbles on the boiling wall
2. The agitation introduced in the flow by the boiling process
3. The diffusion and growth of the bubbles in the flow
4. The interrelationship between bubble distribution and velocity distribution
5. The collapse and agglomeration of bubbles in combination with the existence of different flow regimes.

The system considered is a vertical axi-symmetric boiler. The two phase fluid is assumed to move in a bubbly flow regime in an annular space between a heated inner wall and a non-heated outer wall. The flow enters at the bottom and leaves the boiler at the upper end. Bubbles are supposed to be only generated in crevices on the heated wall which occurs in continuous streams.

The set of three common flow equations based upon the conservation laws, in this study written in a refined form, have been completed by a bubble density distribution equation. Supplementary equations have been formulated in order to describe the number of nucleation sites, the growth of the bubbles at the heated surface, the radial velocity of detached bubbles and the diffusion of bubbles in radial direction.

The introduction of radial coordinates implies temperature-, void-, and

velocity profiles over the cross section and related to this also radially varying values of the local slip. In case it is intended to derive from the fundamental model a so-called "engineering formula", it is required to define two more slipratios than is commonly accepted. This has been argued more in detail in ref.5. It is impossible or at least very difficult to distinguish experimentally between the three slipratios and they can be treated therefore, only theoretically when accepting basic laws concerning bubble behaviour.

Much emphasis in the theory has been put upon the correct representation of the following experimental facts:

1. The large increase in frictional pressure-drop due to the two phase character of the flow.
2. The large increase in heat transfer owing to nucleate boiling.

The set of simultaneous differential equations, obtained for the various unknowns, being too complicated in this state to be treated mathematically, have been made dimensionless and all terms which are essentially smaller than comparable others have been neglected. In the steady state 8 similarity parameters appear to govern the flow process.

In order to evaluate the model, it was considered to be attractive to investigate first whether the derived equations can yield realistic results when programming a somewhat simplified set of equations still maintaining however, the essential properties of the model. This has been done by prescribing the form of the radial distributions of temperature, velocity and number density. The velocity profile has been chosen for instance to be sine-shaped.

Calculations with this model have been carried out for such a combination of power and pressure that bubble flow could be expected to exist in the boiling region. The results are quite encouraging. The calculated values of slip and two phase friction are in close agreement to those obtained from experiments (see ref.5.)^{and fig. 23}). In a further development the radial distributions are no longer prescribed but computed by the set of equations.

6. Future program.

The series experiments under forced convection will be continued after expiration of the present contract. The conditions chosen are saturation temperatures of 120, 200 and 234°C, inlet velocities varying from .6 up to 2 m/sec, zero subcooling. At a condition of 200°C saturation temperature the subcooling will be varied between zero and 15°C at the inlet. During the steady state measurements attention will be paid to pressure differences and void fractions along the channel in order to be able to analyse the results in terms of slipfactor and two phase friction multiplier. Comparison will be made with the measurements obtained earlier under natural circulation.

As far as spontaneous oscillations occur in this damped system, they will be the subject of an extensive study to the character and the threshold of the instabilities.

The stability of the system will be further investigated by applying the technique of transfer functions with disturbance of the power.

A separate series of experiments will be carried out to study the influence of a sine-shaped heat flux on steady state as well as on the dynamic characteristics of the boiling system. Heating elements with a varying wall-thickness will be applied.

The linearized model will be developed further and refined in a sense as is indicated in chapter 2. Attention will be paid to the correct prediction of the effect of subcooling.

In a further development of the model based upon first principles the radial distributions of temperature, phase velocity and number density are no longer prescribed but computed by the set of equations.

7. References.

1. Spigt, C.L., On the hydraulic characteristics of a boiling water channel with natural circulation. Report WW-R92, 1966.
2. Dijkman, F.J.M., Tummers, J.F., Spigt, C.L., The stability characteristics of a boiling system with natural and forced circulation. Report WW-R 124, 1967.
3. Bowring, R.W., Physical model, based on bubble detachment, and calculation of steam-voidage in the subcooled region of a heated channel, Report OECD Halden Reactor Project, HPR 10, 1962.
4. Verheugen, A.N.J., Dijkman, F.J.M., Lamein, H.J., Tong, L.S., The influence of the response characteristics of the heating rod on the stability and burn out characteristics of a boiling channel. Report WW-R125, 1967.
5. Van der Walle, F., Spigt, C.L., Bogaardt, M., Verheugen, A.N.J., A theoretical study on two phase flow characteristics. Report WW-R122, 1967.

List of Special Technical Reports.

1. Spigt, C.L., Simon Thomas, J.P., Bogaardt, M., Introductory laboratory studies of boiling reactor stability, October 1961, Report WW016-R10.
2. Van der Walle, F., Study of possible application of acoustical methods for determining void fraction in boiling water reactors, 1962, Report WW016-R11.
3. Spigt, C.L., Results of burn out and instability experiments on a 7-rod bundle at up to 30 atmospheres pressure and under conditions of natural convection and zero inlet subcooling, Report WW016-R21.
4. Tummers, J.F., Spanjers, Th. Results of flowrate measurements on a 7-rod bundle element with natural circulation and with inlet subcooling up to 30 atm pressure, Report WW016-R26.
5. Spigt, C.L., Instability and burn out observations made during a development of a burn out detector, 1962, Report WW016-R27.
6. Van der Walle, F., Special technical report on the design of an experimental acoustical set-up, 1963, Report WW016-R28.
7. Bowring, R.W., Spigt, C.L., Halden II 7-rod bundle stability and burn out tests up to 30 atm. pressure - second series with natural convection and inlet subcooling, Report WW016-R31.
8. Spigt, C.L., Bogaardt, M., Some burn out and instability experiments on a 7-rod cluster, Report WW016-R48.
9. Spigt, C.L., Dijkman, F.J.M., Callen, J.D., Bogaardt, M., Theoretical and experimental results on steady state boiling in an annular geometry, Report WW016-R52.
10. Spigt, C.L., Dijkman, F.J.M., Bogaardt, M., The onset of hydraulic instabilities in an annular channel, Report WW016-R53.
11. Van der Walle, F., Lamein, H.J., On the hydrodynamic aspects of two phase flows in vertical boilers, Report WW016-R50.
12. Van der Walle, F., Lamein, H.J., Spigt, C.L., Bogaardt, M., A new model of two phase flow in vertical boilers, Report WW016-R54.
13. Dijkman, F.J.M., Spigt, C.L., Bogaardt, M., Les phénomènes accompagnant le début de l'instabilité de l'écoulement dans des canaux verticaux bouillants, Report WW016-R57.
14. Bogaardt, M., Spigt, C.L., Dijkman, F.J.M., Madsen, N., Heat transfer and stability in boiling water reactors, Report WW016-R60.

15. Bowring, R.W., Spigt, C.L., 7-Rod bundle natural circulation stability and burn out tests with water at up to 30 atm. pressure, Report WW016-R68.
16. Bogaardt, M., Spigt, C.L., Some results of measurements in steady and non-steady state in an annular geometry obtained in the two phase flow programme of the laboratory of heat transfer and reactor engineering of the Technological University of Eindhoven, Report WW016-R69.
17. Spigt, C.L., Wamsteker, A.J.J., Van Vlaardingen, H.F., The application of the impedance method for transient void fraction measurement and comparison with the γ -ray attenuation technique, Report WW016-R66.
18. Spigt, C.L., Wamsteker, A.J.J., Van Vlaardingen, H.F., Review of the measuring, recording and analyzing methods in use in the two phase flow programme of the laboratory of heat transfer and reactor engineering of the technological university of Eindhoven, Report WW016-R64.
19. Anonymous, Kinetics of boiling hydraulic loops, a digital programme for the calculation of non-steady two phase flow in a vertical boiler, based on a model of Jahnberg, Report WW016-R76.
20. Anonymous, Determination of power spectra and transfer functions from digital processing of measuring signals, Report WW016-R77.
21. Van der Walle, F., Verheugen, A.N.J., Haagh, V.J.M., Bogaardt, M., A study of the application of acoustical methods for determining void fractions in boiling water systems, Report WW016-R98.
22. Van der Walle, F., Spigt, C.L., Lamein, H.J., Bogaardt, M., A theoretical study on two phase flow characteristics, Report WW016-R99.
23. Bogaardt, M., Spigt, C.L., Dijkman, F.J.M., Verheugen, A.N.J., On the heat transfer and fluid flow characteristics in a boiling channel under conditions of natural convection, Report WW016-R82.
24. Bowring, R.W., Spigt, C.L., Seven-rod bundle, natural circulation stability and burn out tests with water at up to 28 atm. pressure, Report WW016-R85.
25. Bogaardt, M., Spigt, C.L., Dijkman, F.J.M., Verheugen, A.N.J., Comparison of results of analysis of boiling system dynamics by analog and digital methods, April 1965, Report WW016-R90.

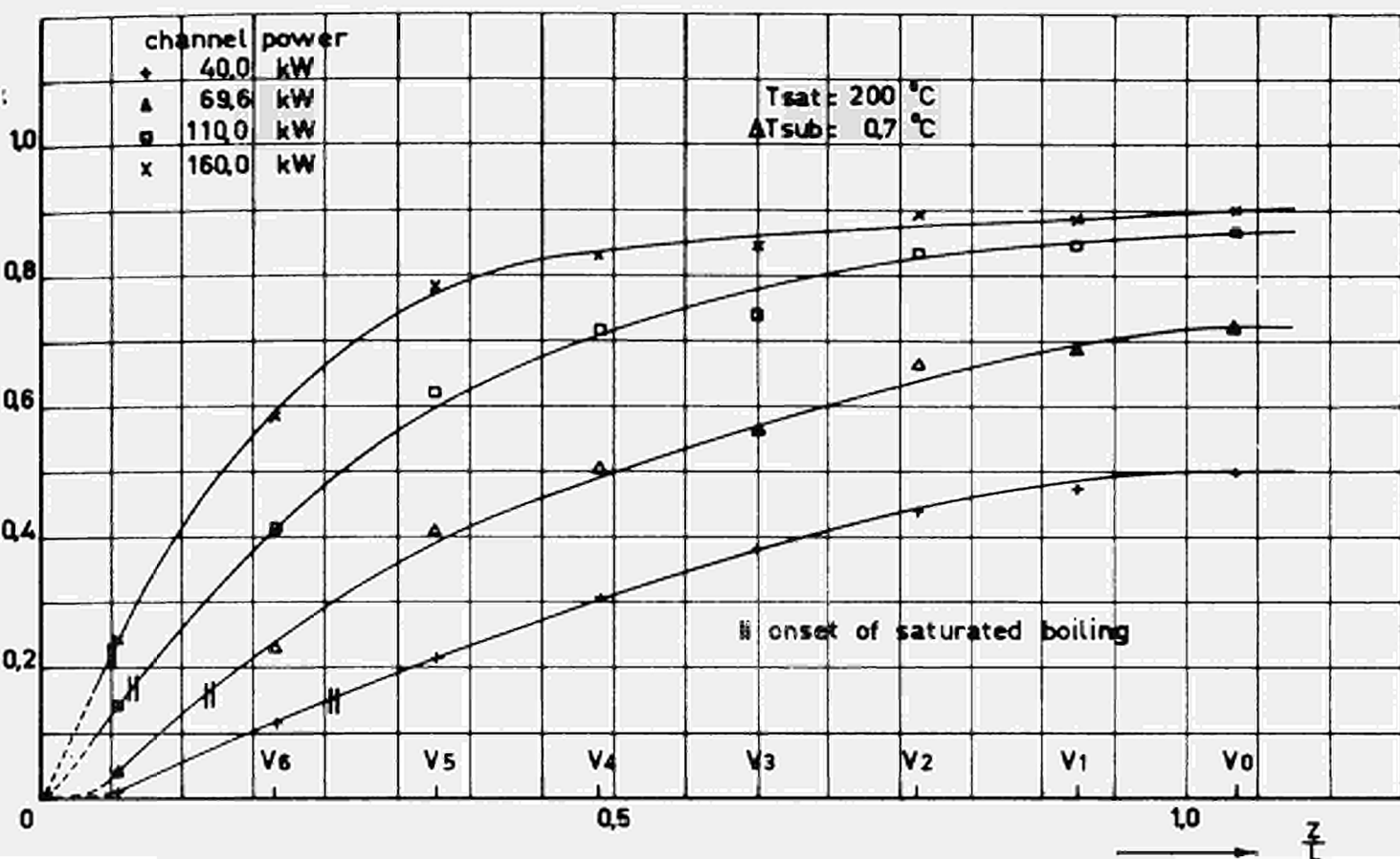


Fig. 1 The longitudinal void fraction distribution for various channel powers, Test Section I.

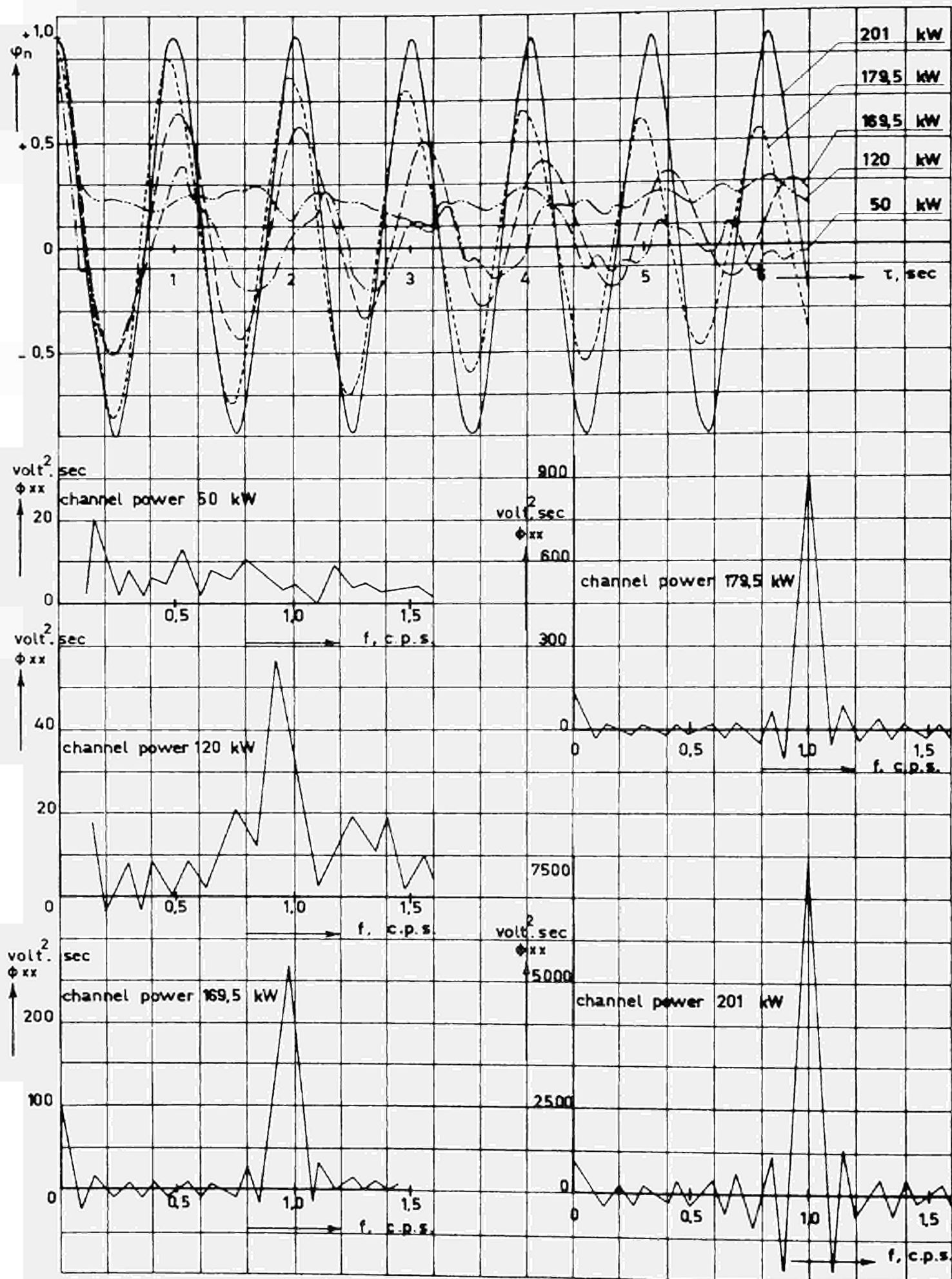


Fig. 2 Autocorrelations and spectral power densities of the $\Delta Pinlet$ signal.

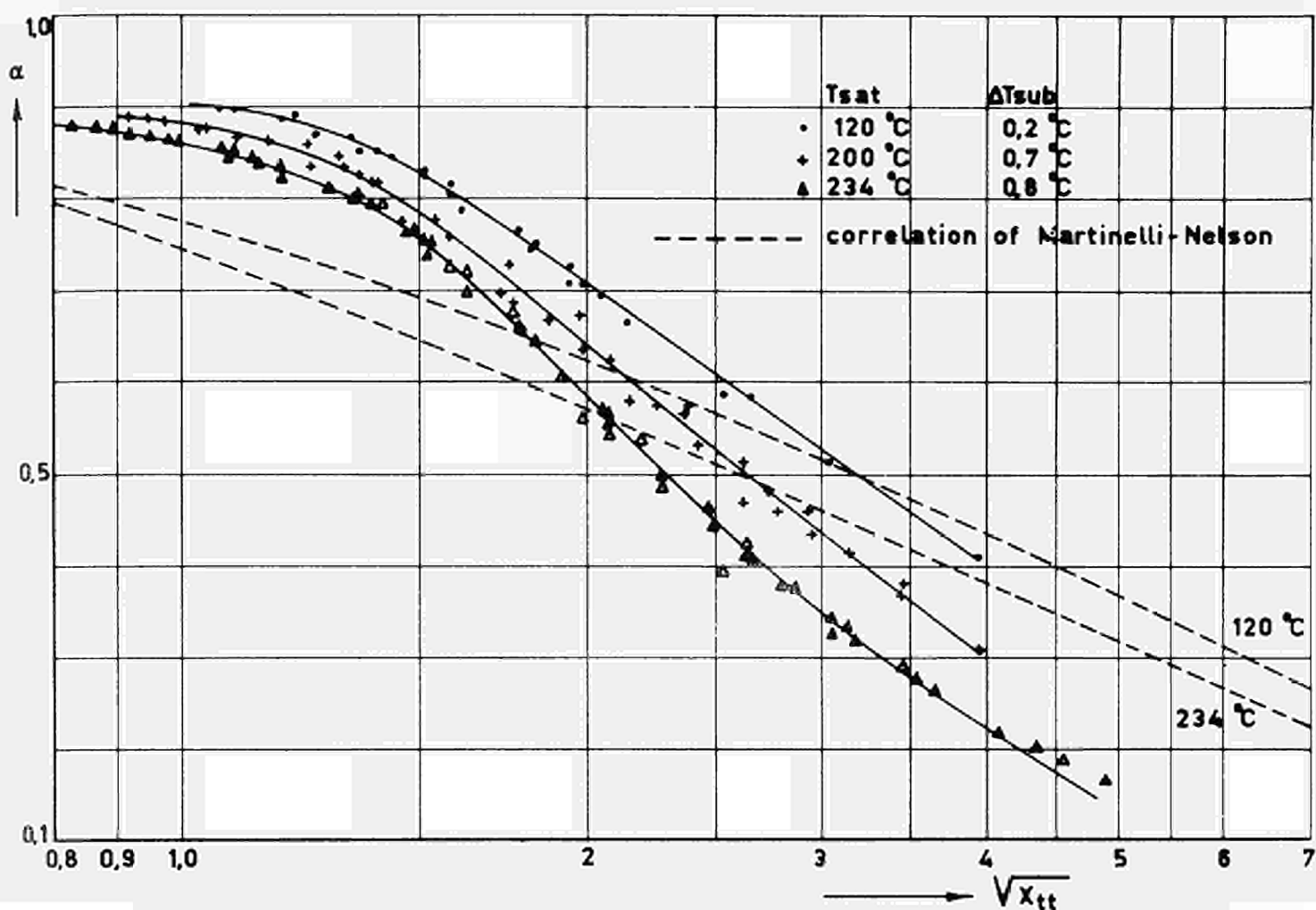


Fig. 3 Void fraction data plotted according to Martinelli-Nelson (M3) for three system pressures, Test Section I.

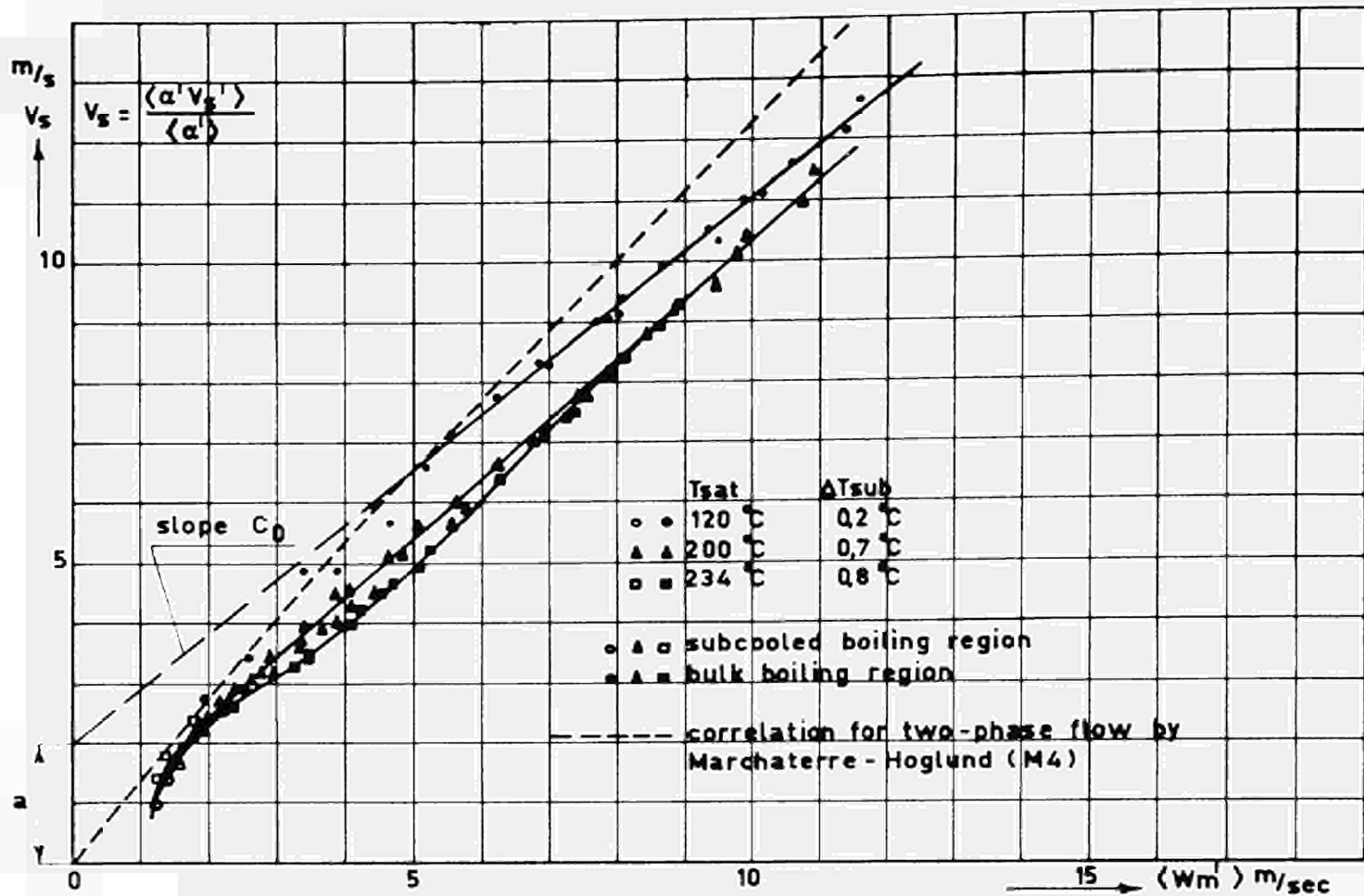


Fig. 4 Void fraction data plotted according to Zuber and Findlay (Z1) for three system pressures, Test Section I.

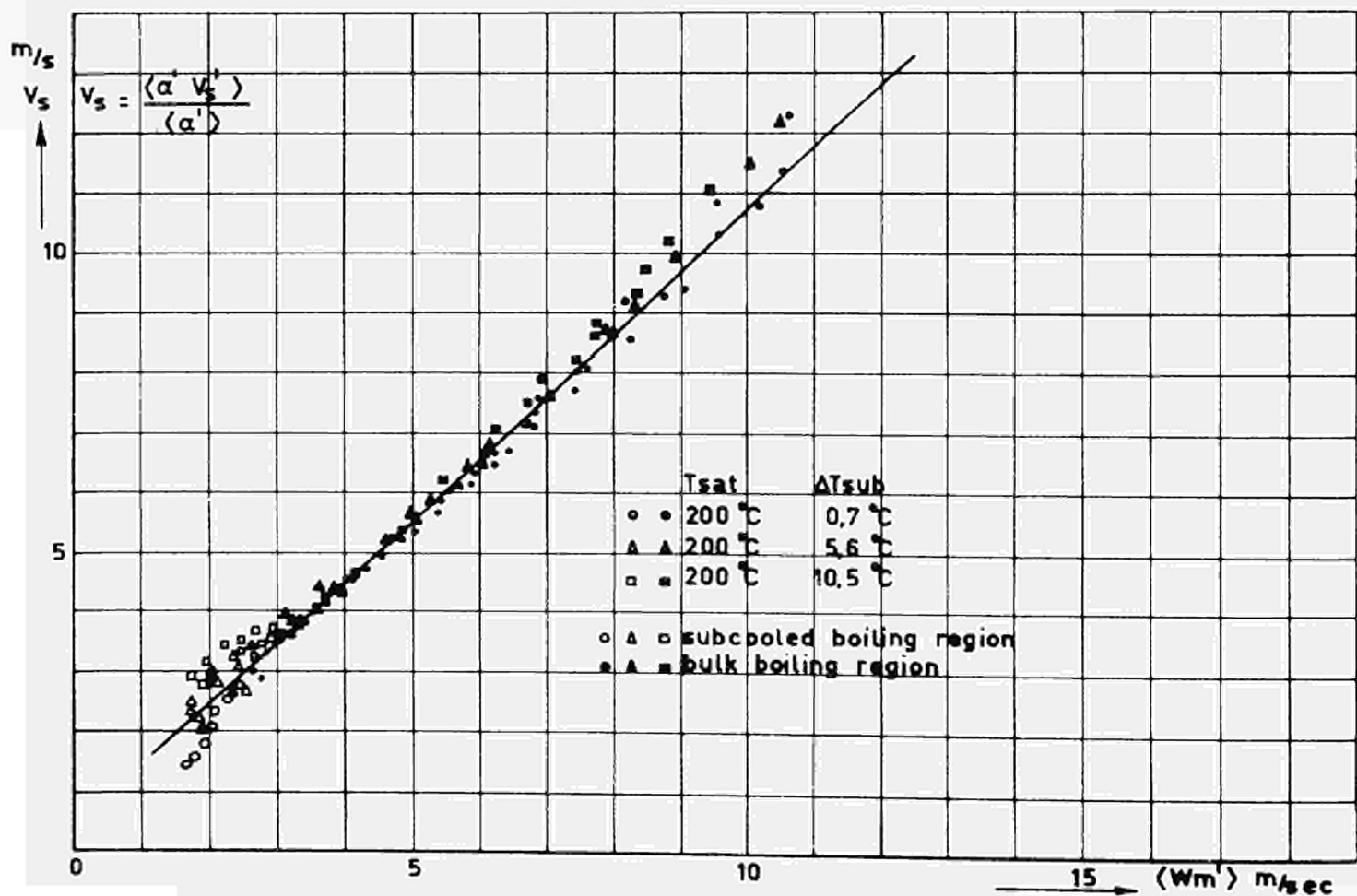


Fig. 4.4 Void fraction data plotted according to Zuber and Findlay (Z1) for three subcooling temperatures, Test Section II.

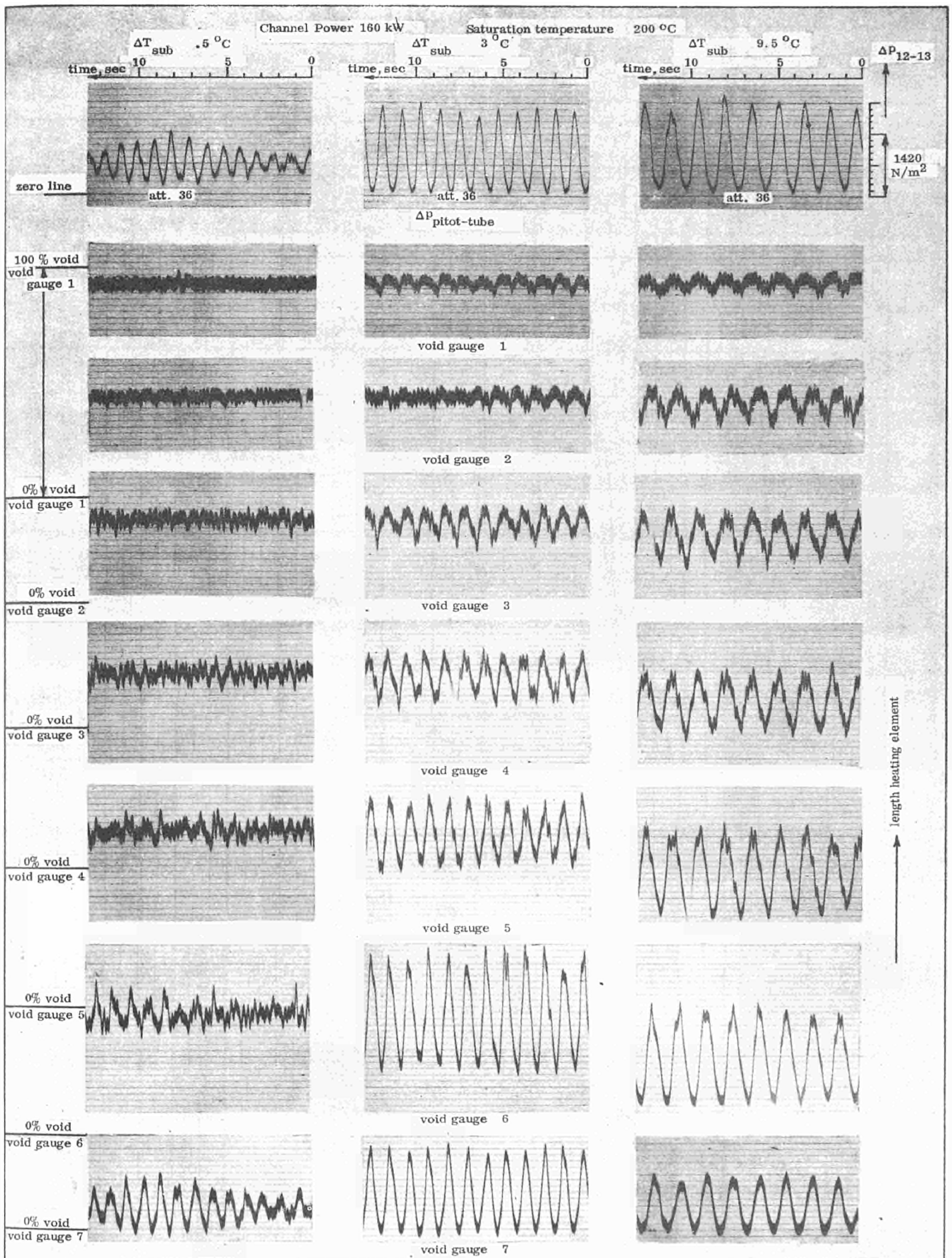


Fig. 5 Recordings of the signals from the pitot tube and various voidgauges under natural circulation.

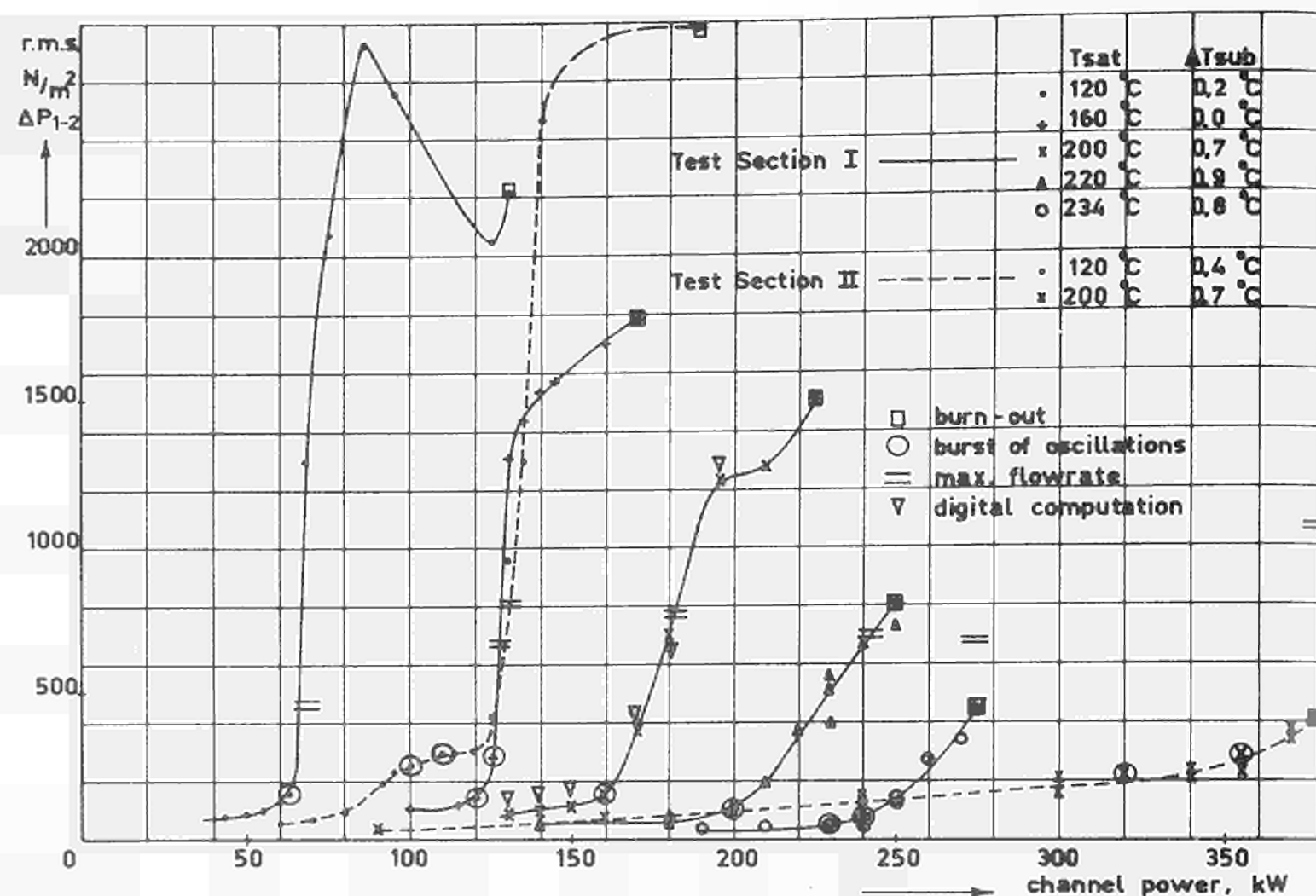


Fig. 6

The influence of system pressure on the onset of hydraulic instabilities.

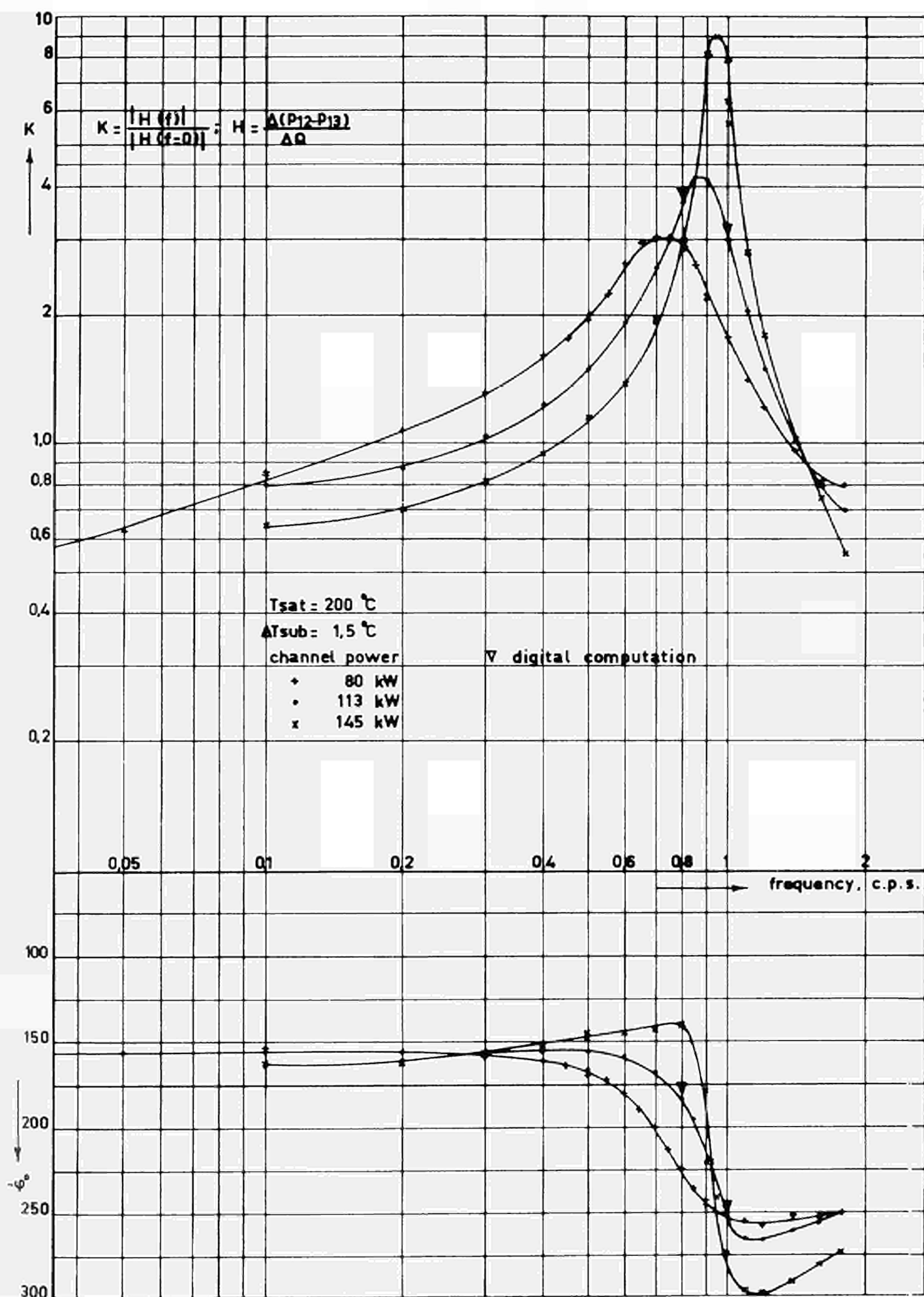


Fig. 7

Transfer functions from channel power to inlet mass flow for various channel powers, Test Section I.

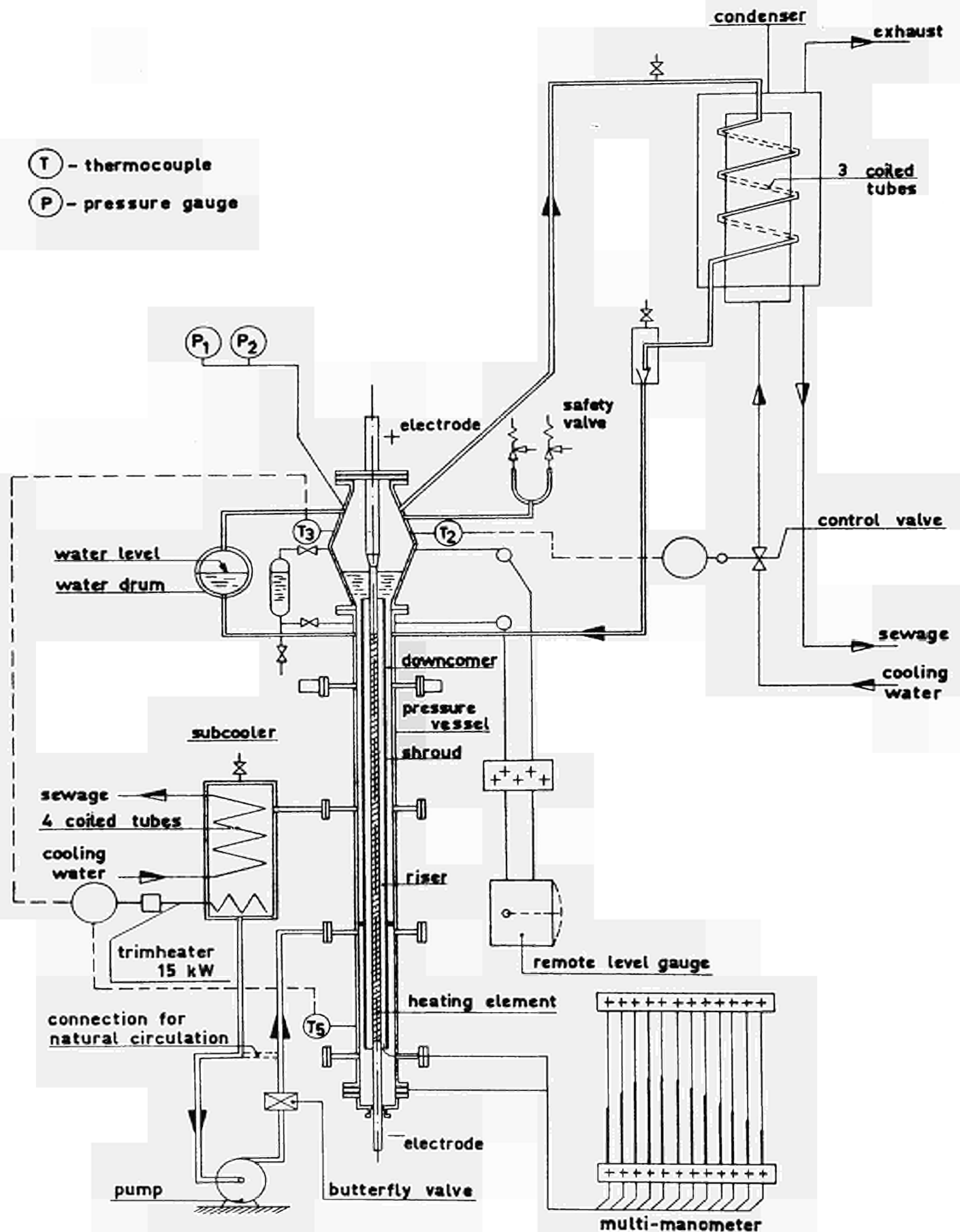


FIG. 8 Flow sheet of the pressurized boiling water loop.

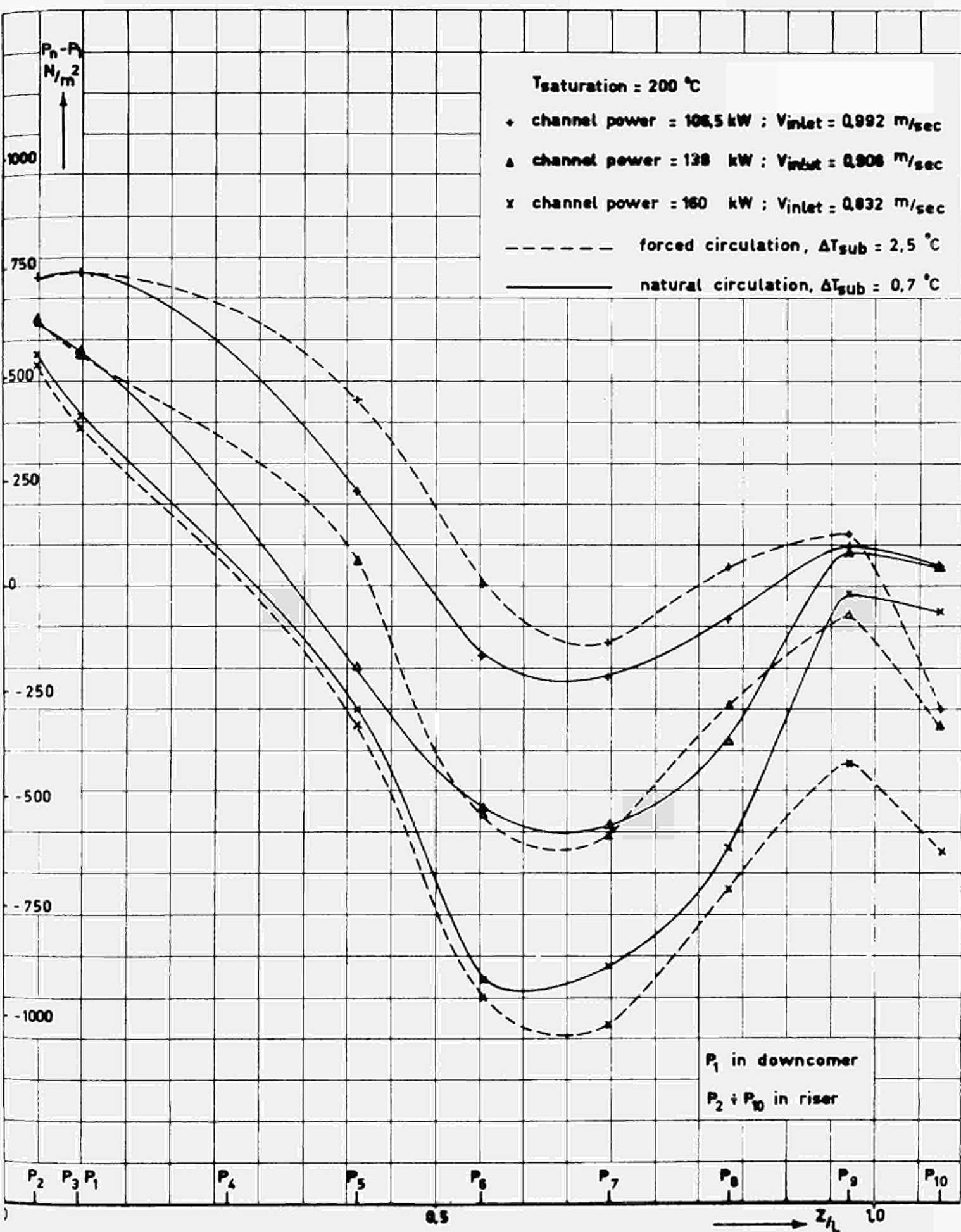


Fig. 9 The longitudinal pressure distribution at three channel powers for forced circulation and natural circulation.

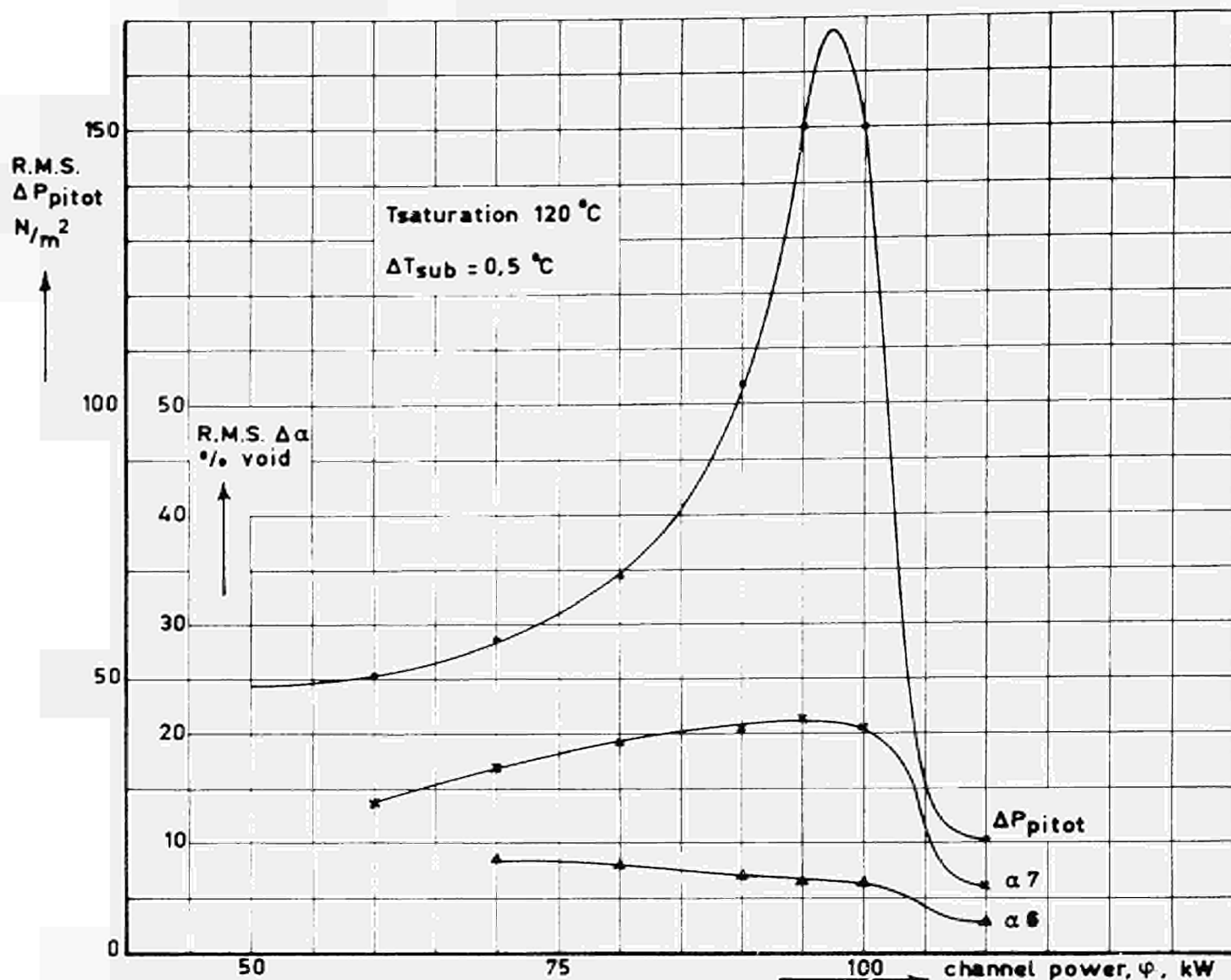


Fig.10a Thresholds of instabilities from the signals of the pitot tube and the void gauges at forced circulation, inlet flowrate nearly zero.

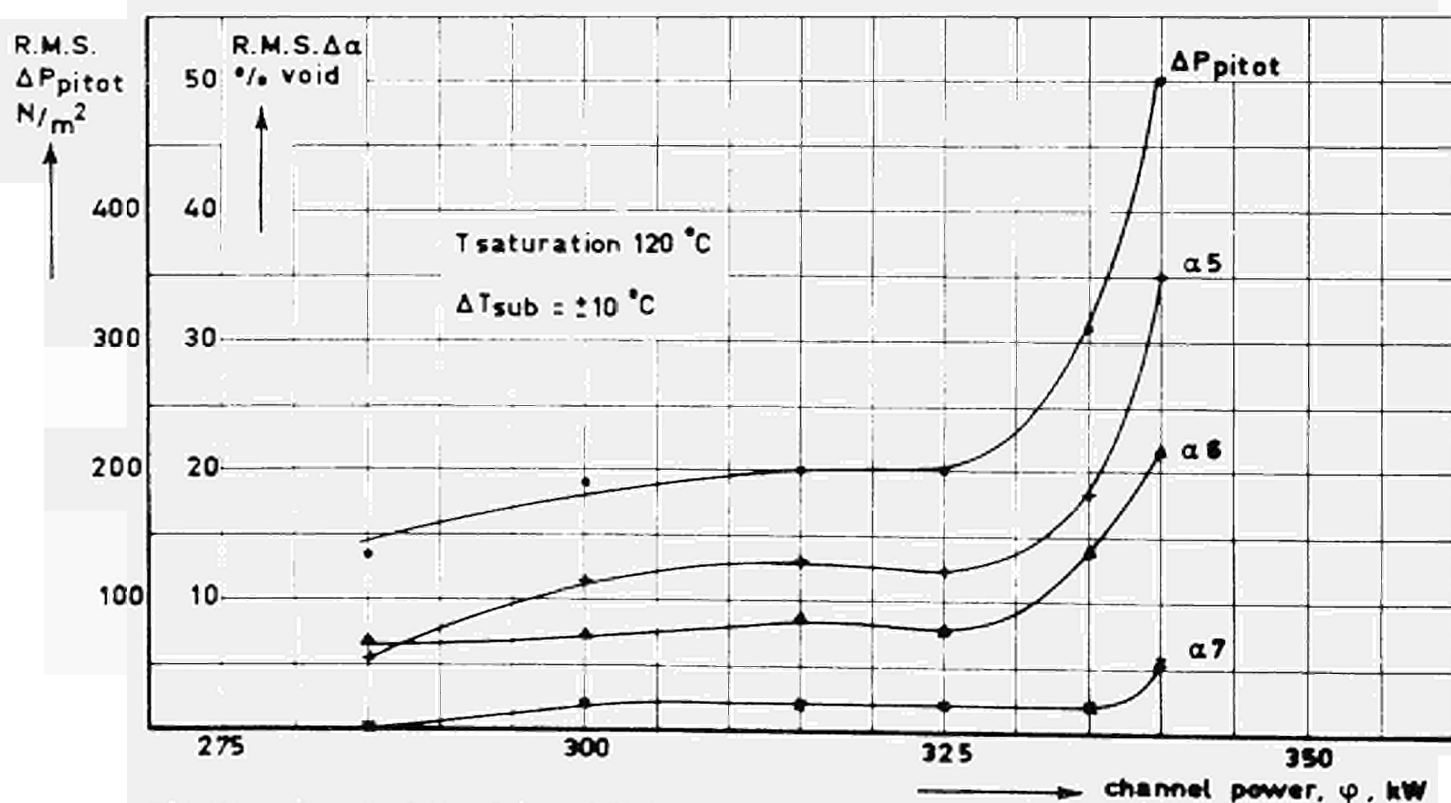


Fig.10b Thresholds of instabilities from the signals of the pitot tube and the void gauges at forced circulation, inlet flowrate 1.5 m/sec.

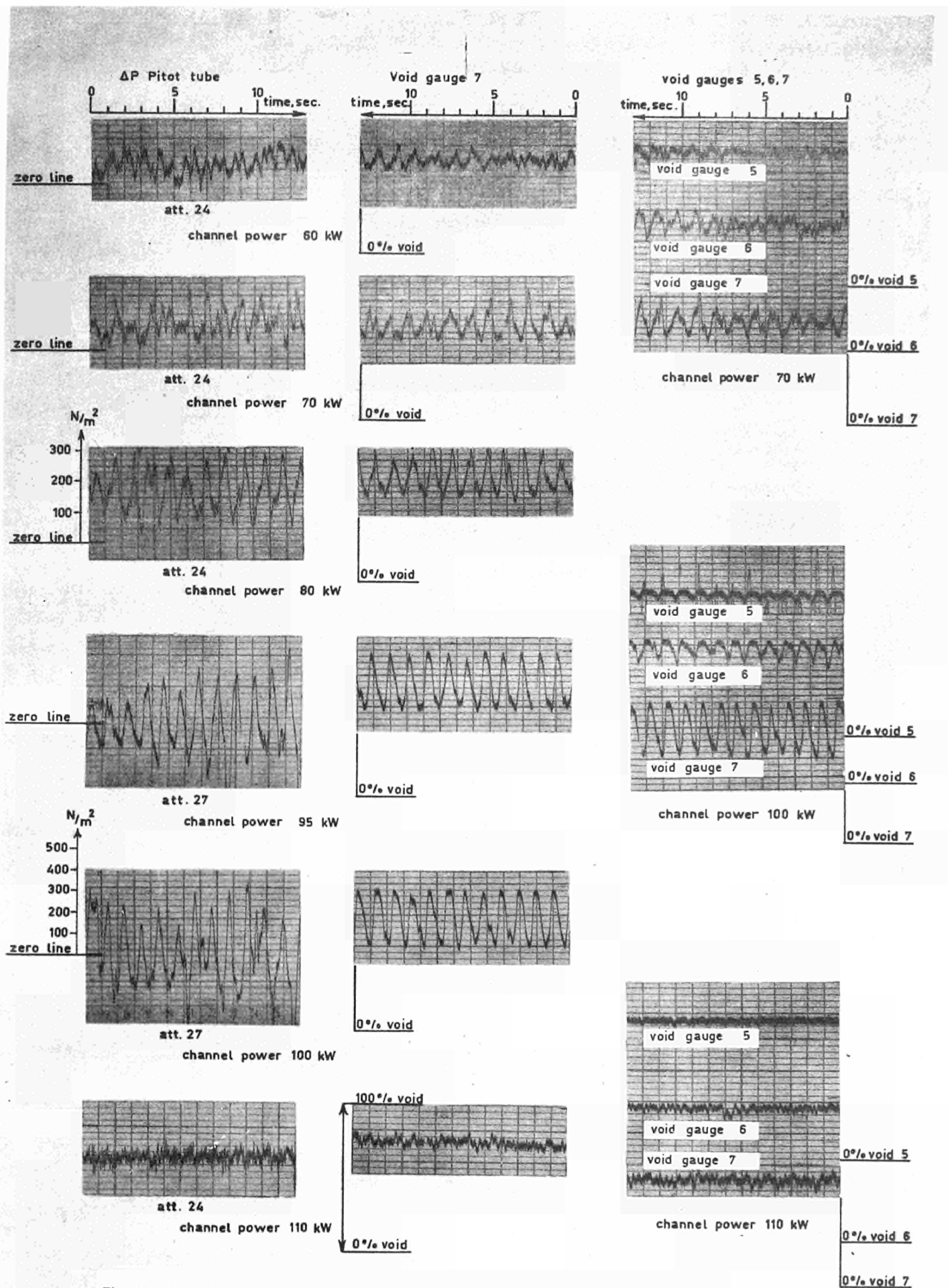


Fig. 11 Recordings of the signals from the pitot tube and various void gauges under forced circulation; saturation temperature 120 °C; inlet flowrate nearly zero; ΔT_{sub} 0.5 °C.

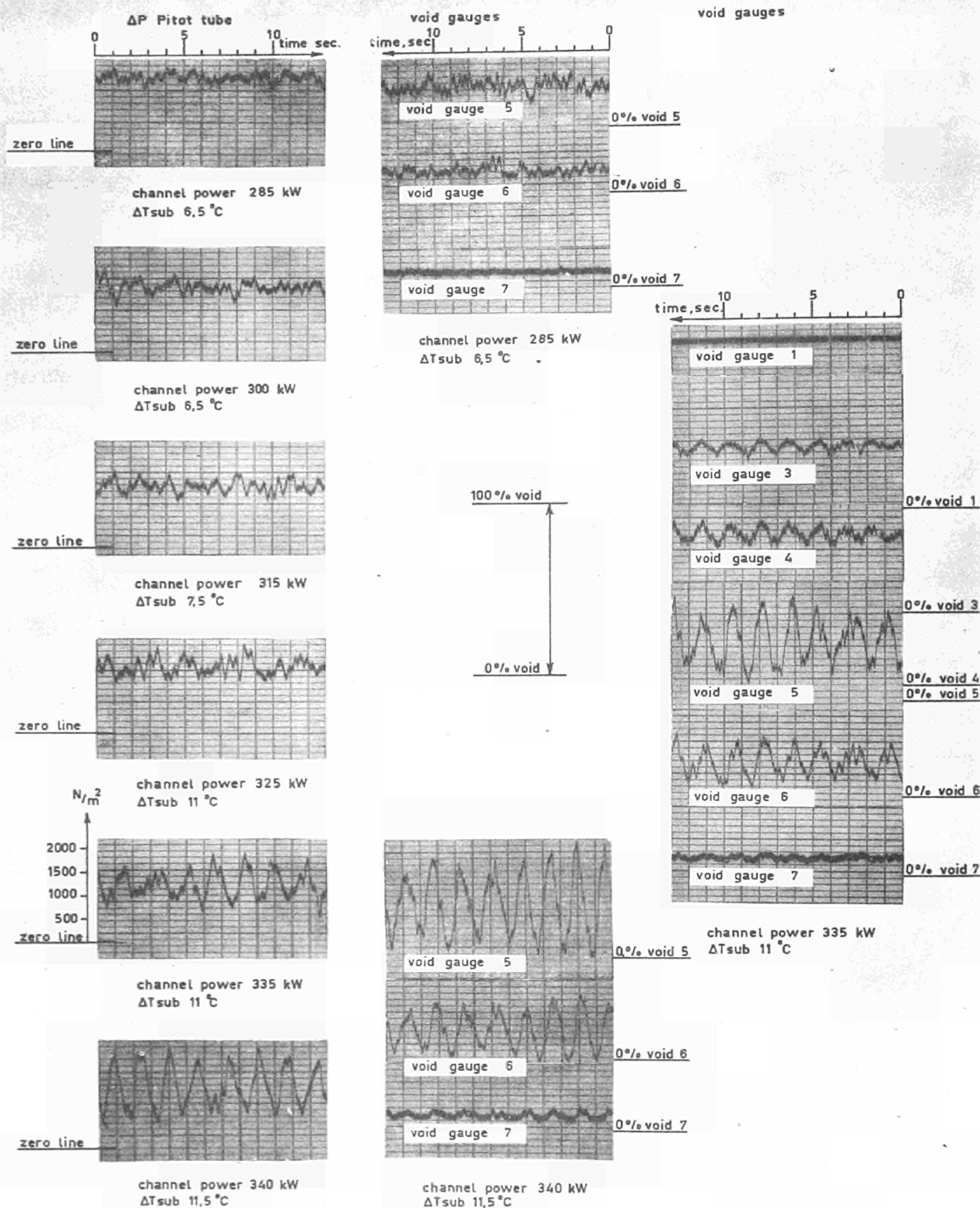


Fig. 12 Recordings of the signals from the pitot tube and various void gauges under forced circulation; saturation temperature 120 °C; inlet flowrate 1,5 m/sec.

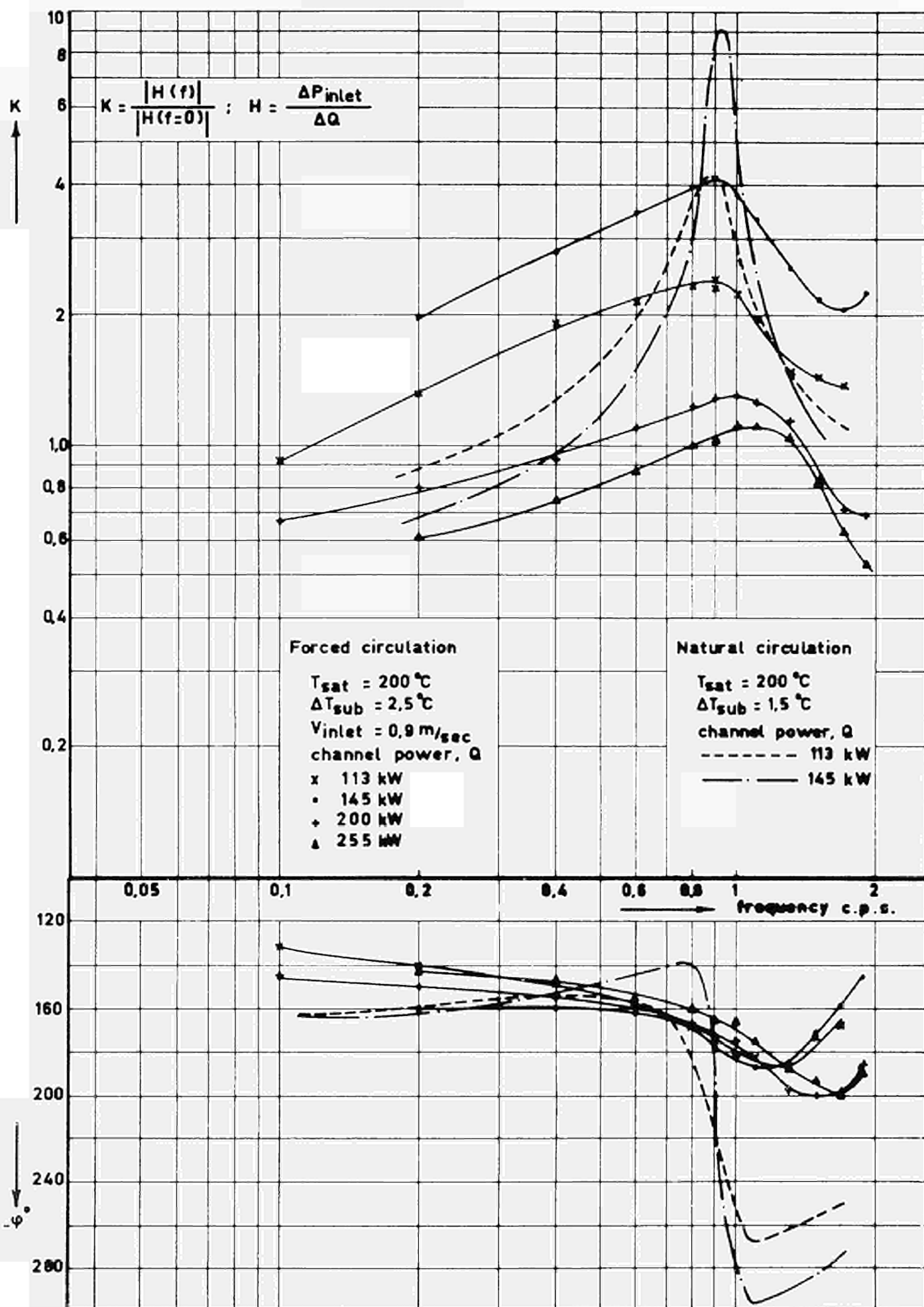


Fig. 13 Transfer functions from channel power to inlet mass flow for various channel powers.

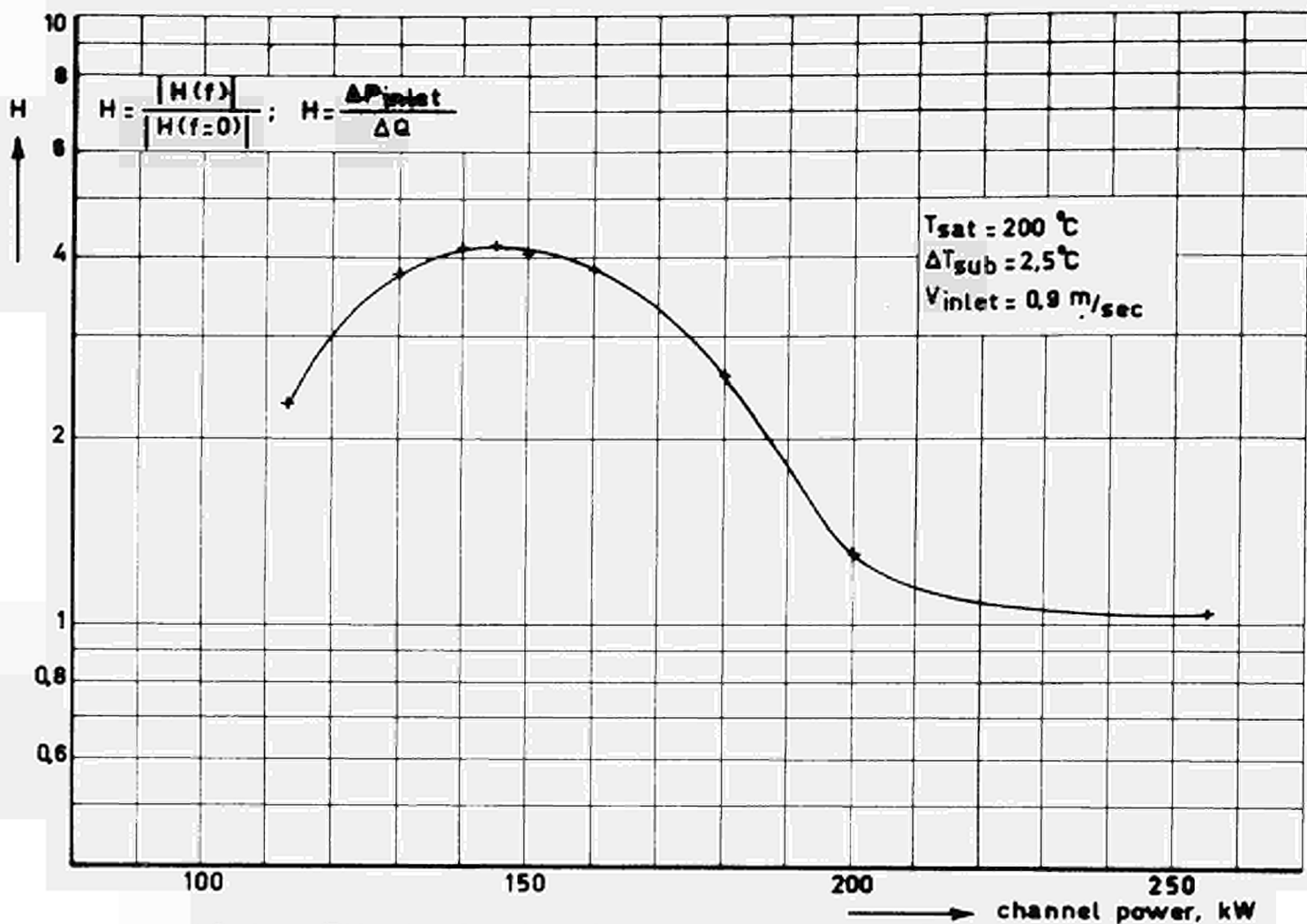


Fig. 14 Transfer function from channel power to inlet mass flow at a constant frequency (0.9 Hz.) and different power levels under forced circulation.

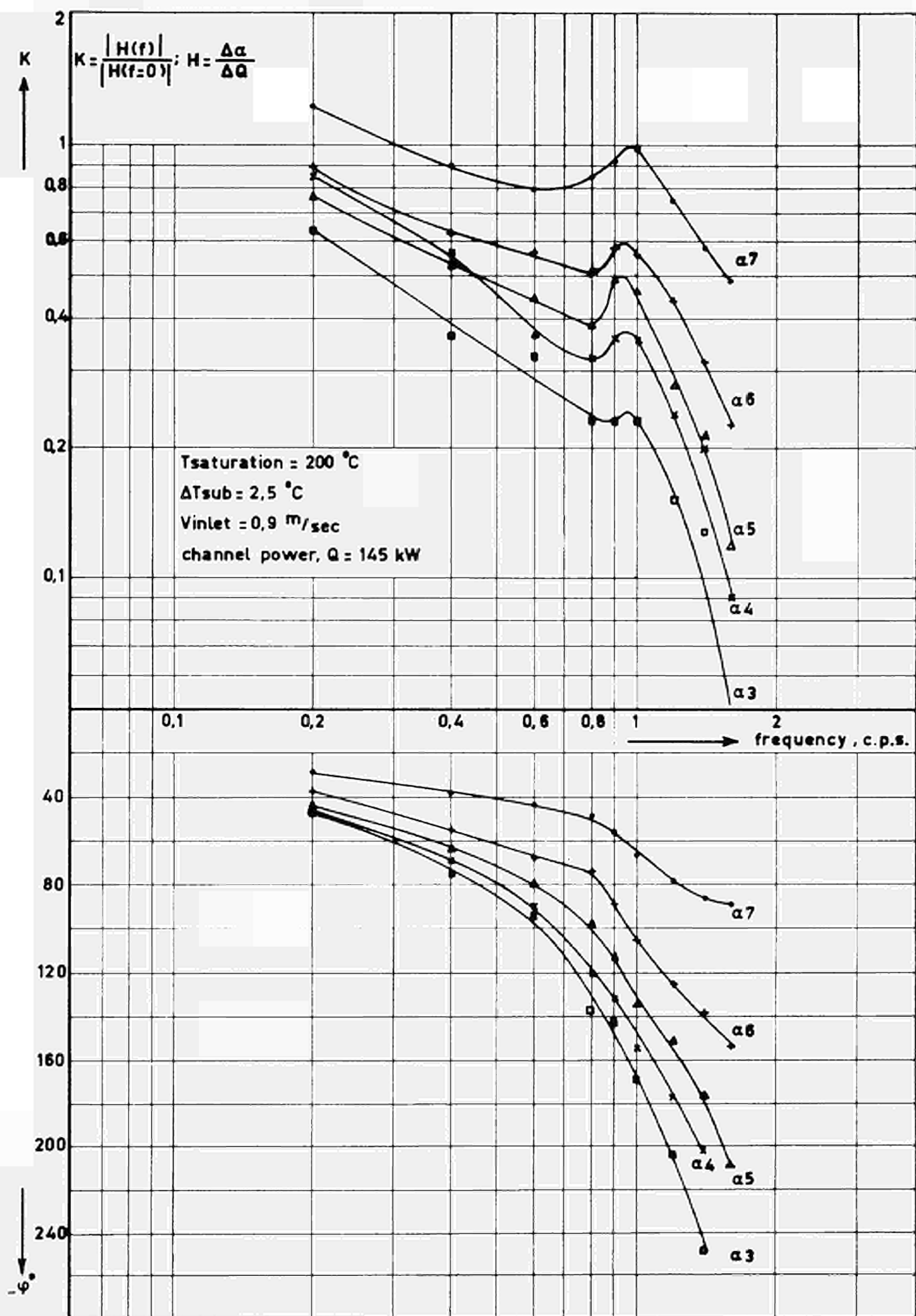


Fig. 15 Transfer functions from channel power to the void fraction at different locations under forced circulation.

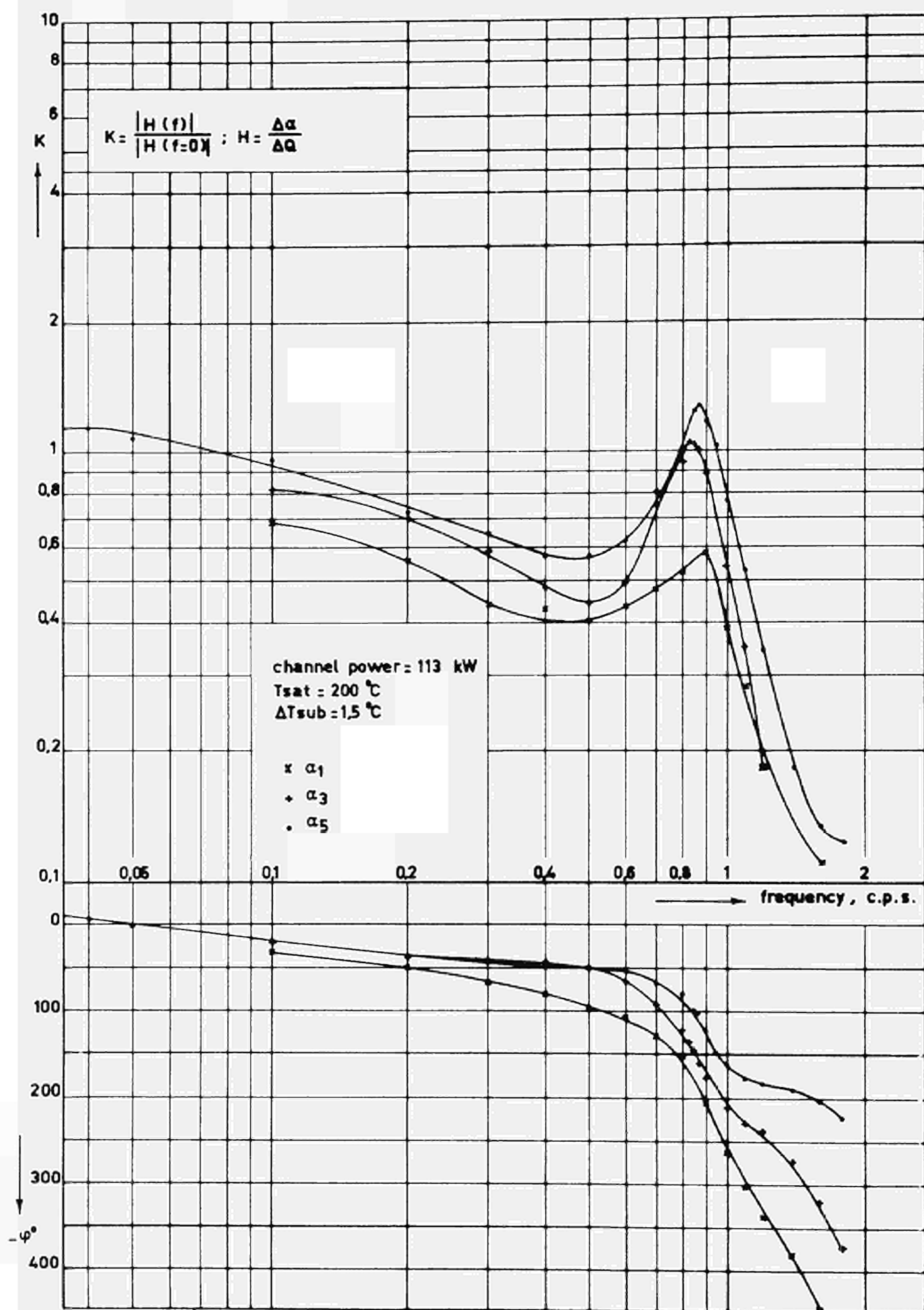


Fig.16

Transfer functions from channel power to the void fraction at different locations, under natural circulation.

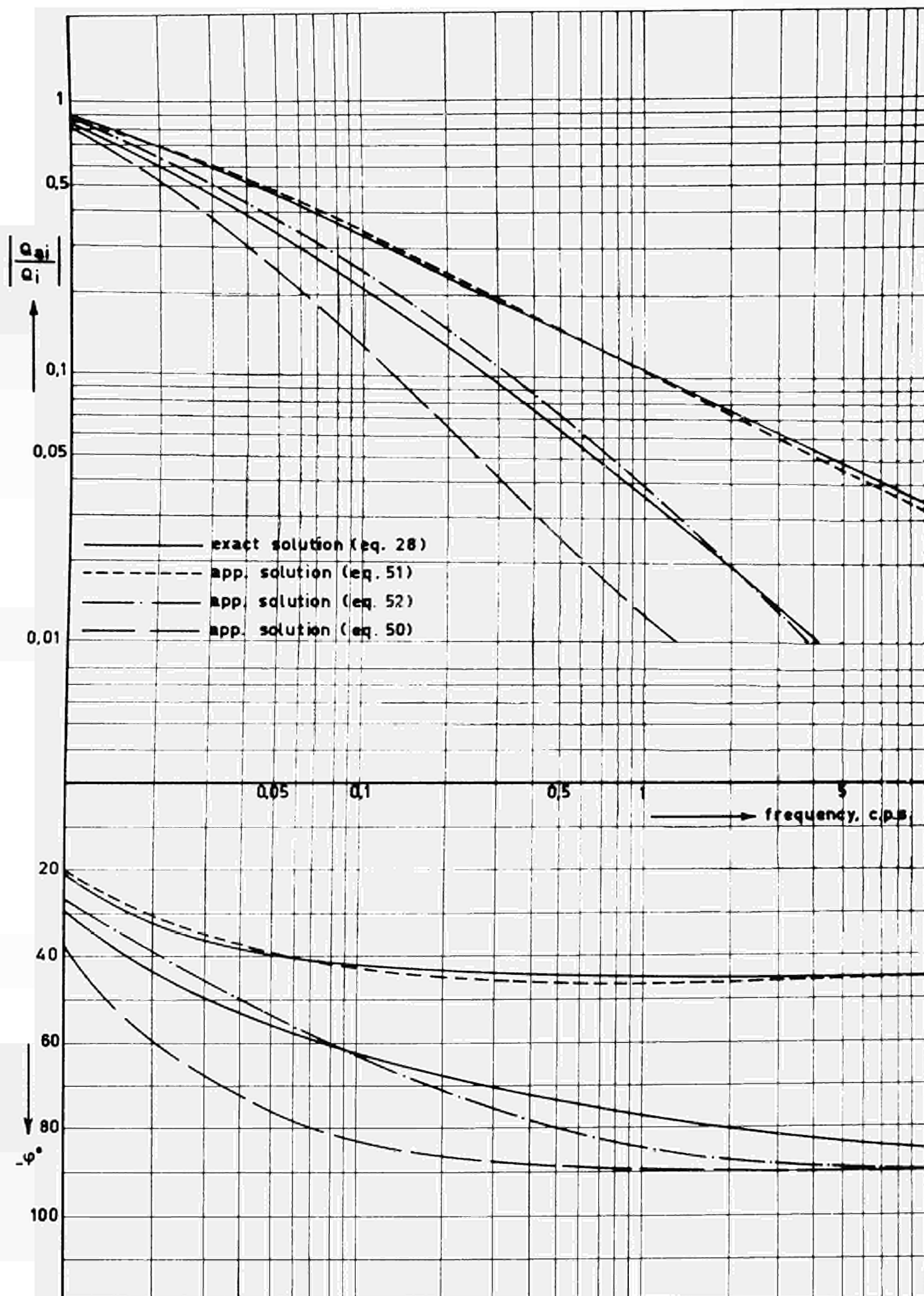


Fig. 17 Approximated transfer functions of the electrically heated solid bar from equations (50), (52) and (53) compared with the exact solution.

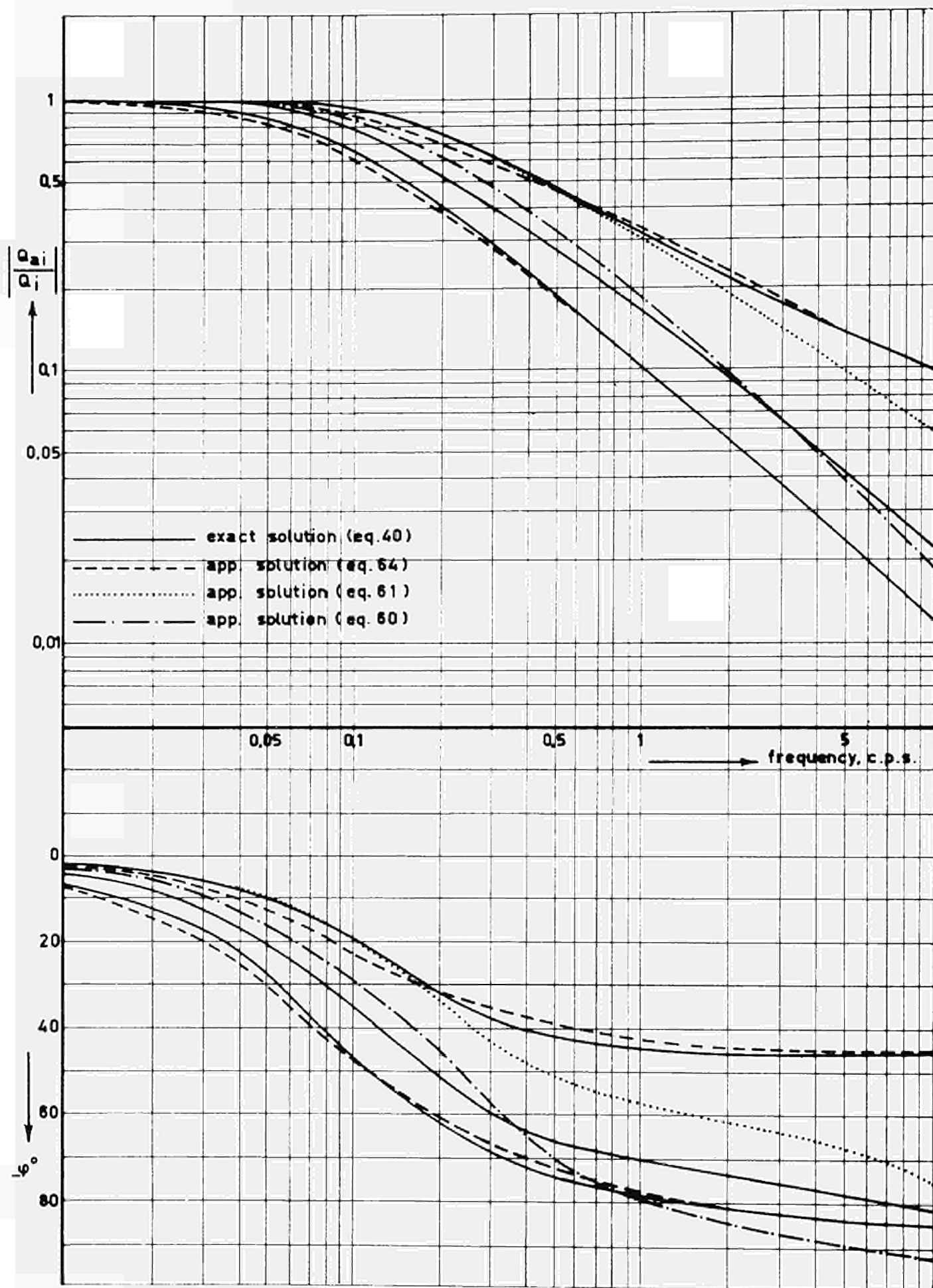


Fig. 18 Approximated transfer functions of the tube from equations (60), (61) and (64) compared with exact solution.

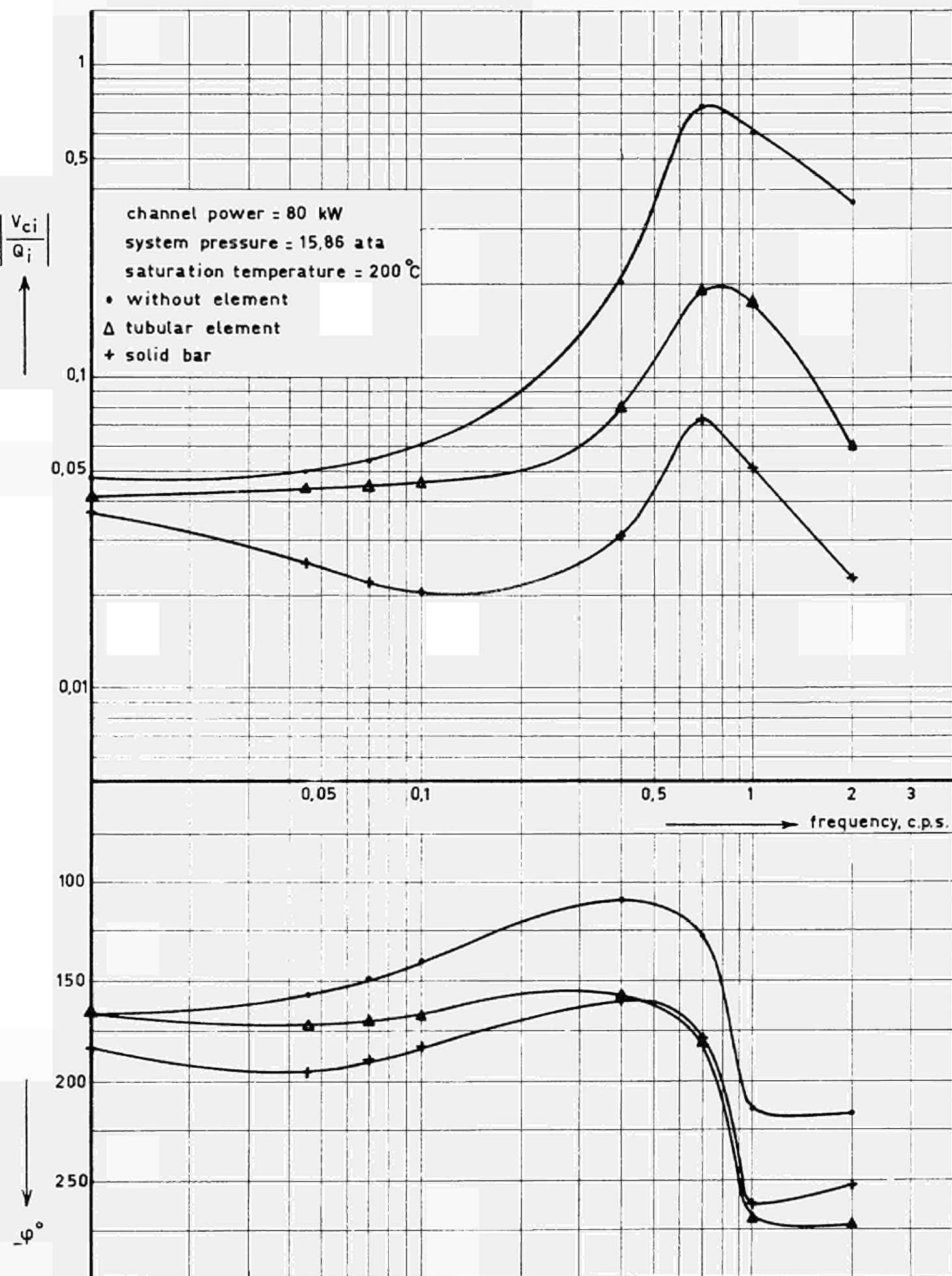


Fig. 19 Amplitude (dimensionless) and phase from the transfer function from channel power to inlet velocity for different heating

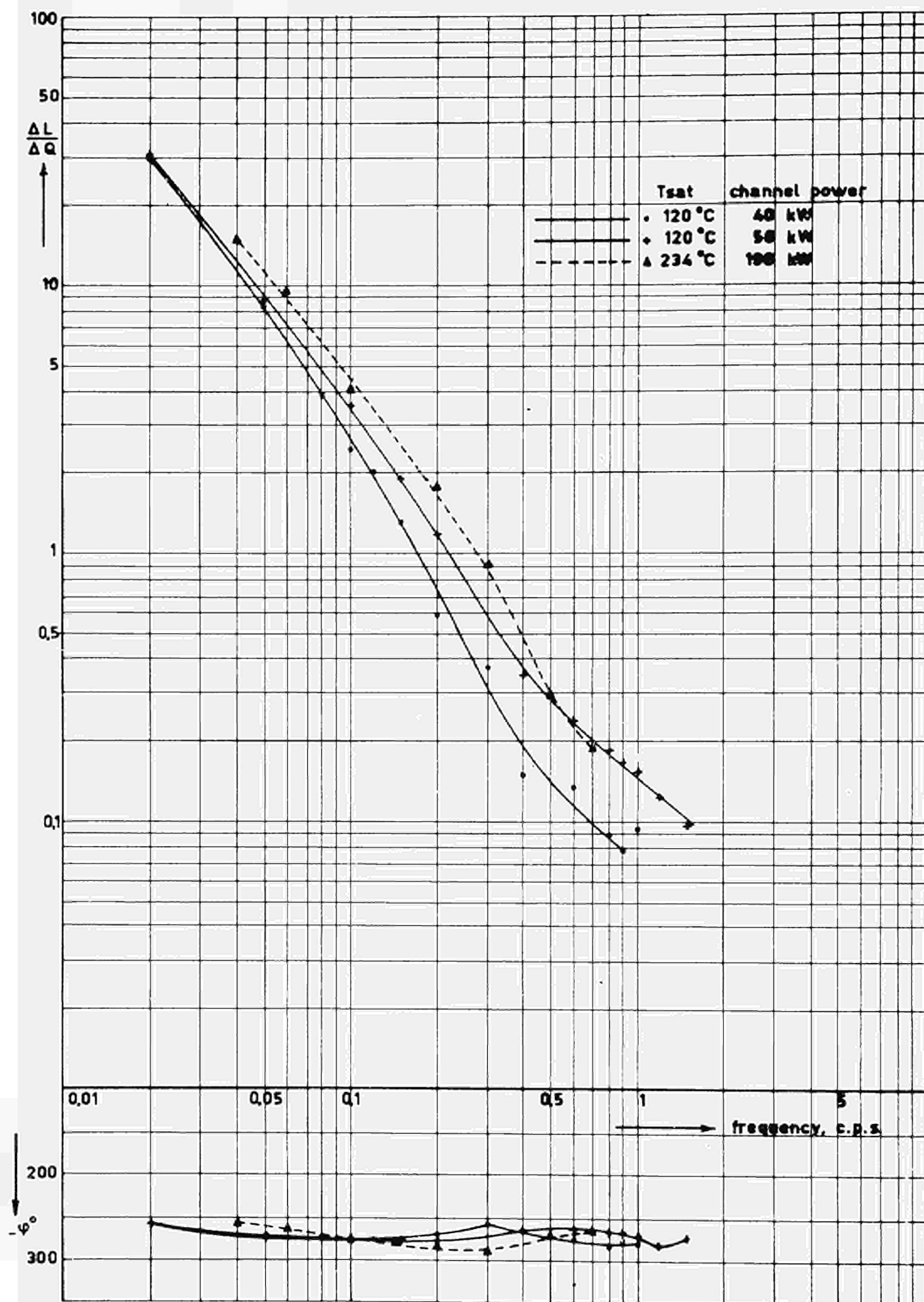


Fig. 20 Transfer function from channel power to elongation of the heating element (solid bar) at three system pressures, natural circulation.

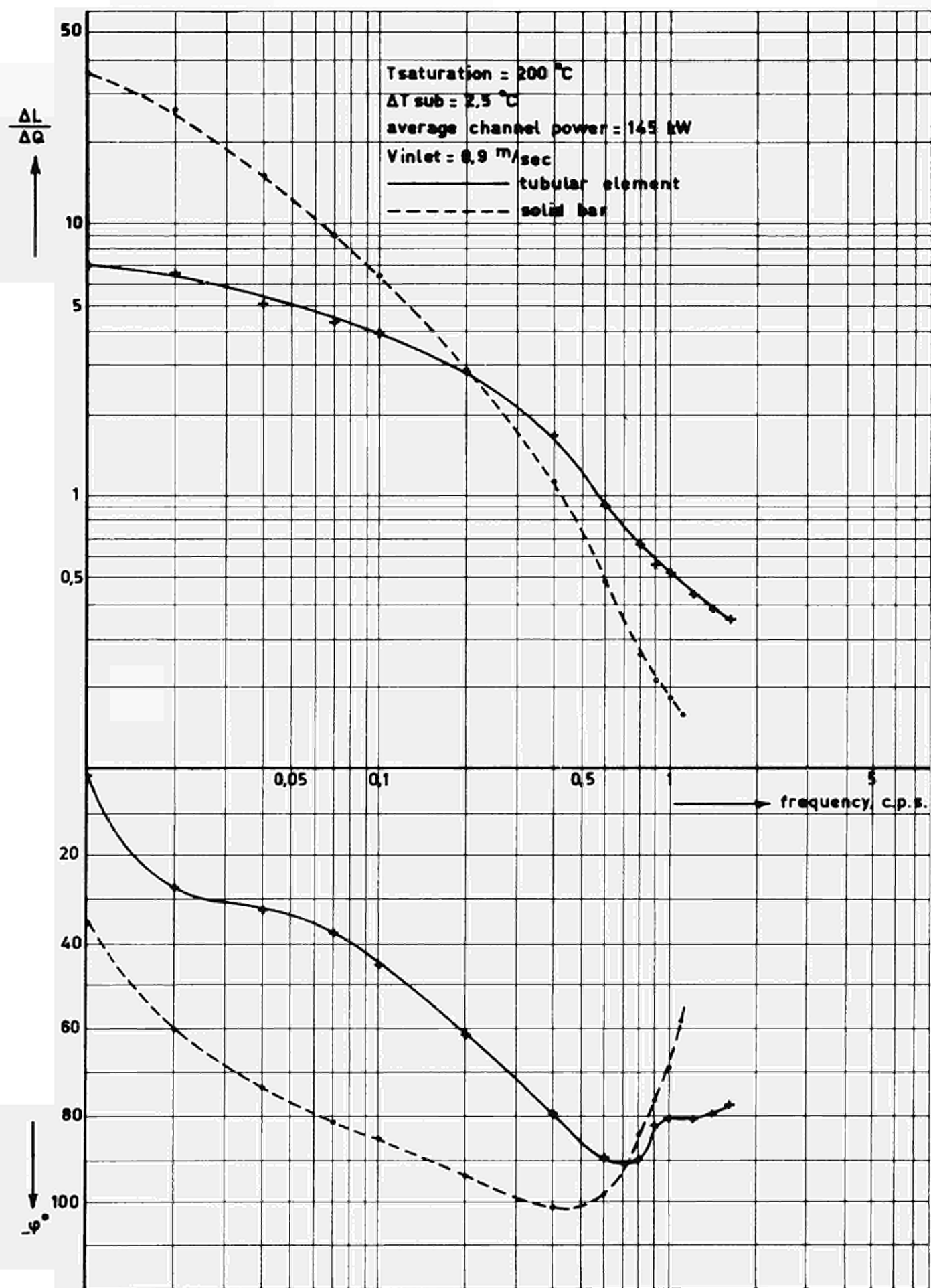


Fig. 21 Transfer function from channel power to elongation for a solid bar and tube in forced circulation.

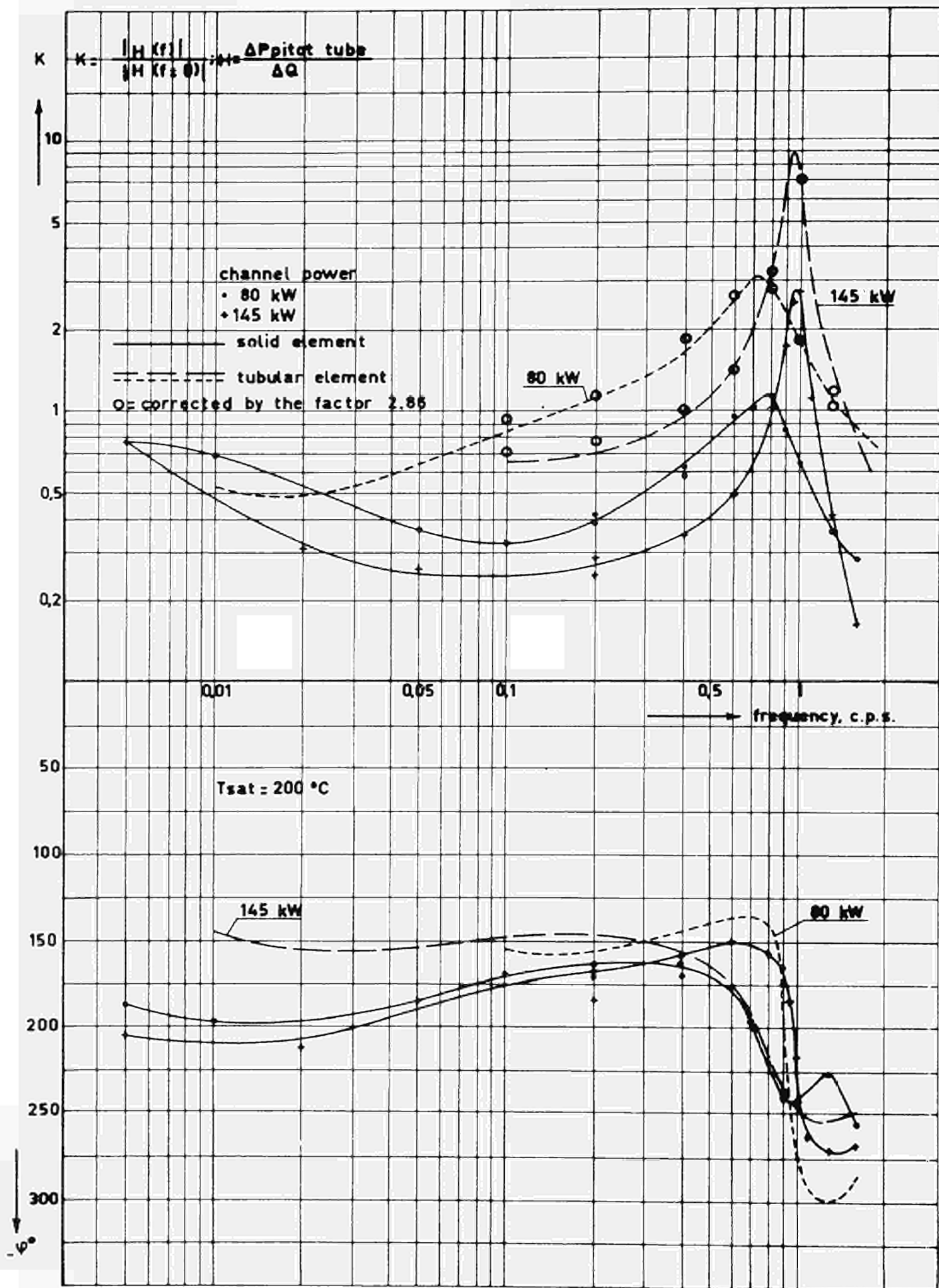


Fig. 22 Transfer function from channel power to inlet mass flow for two channel powers, natural circulation.

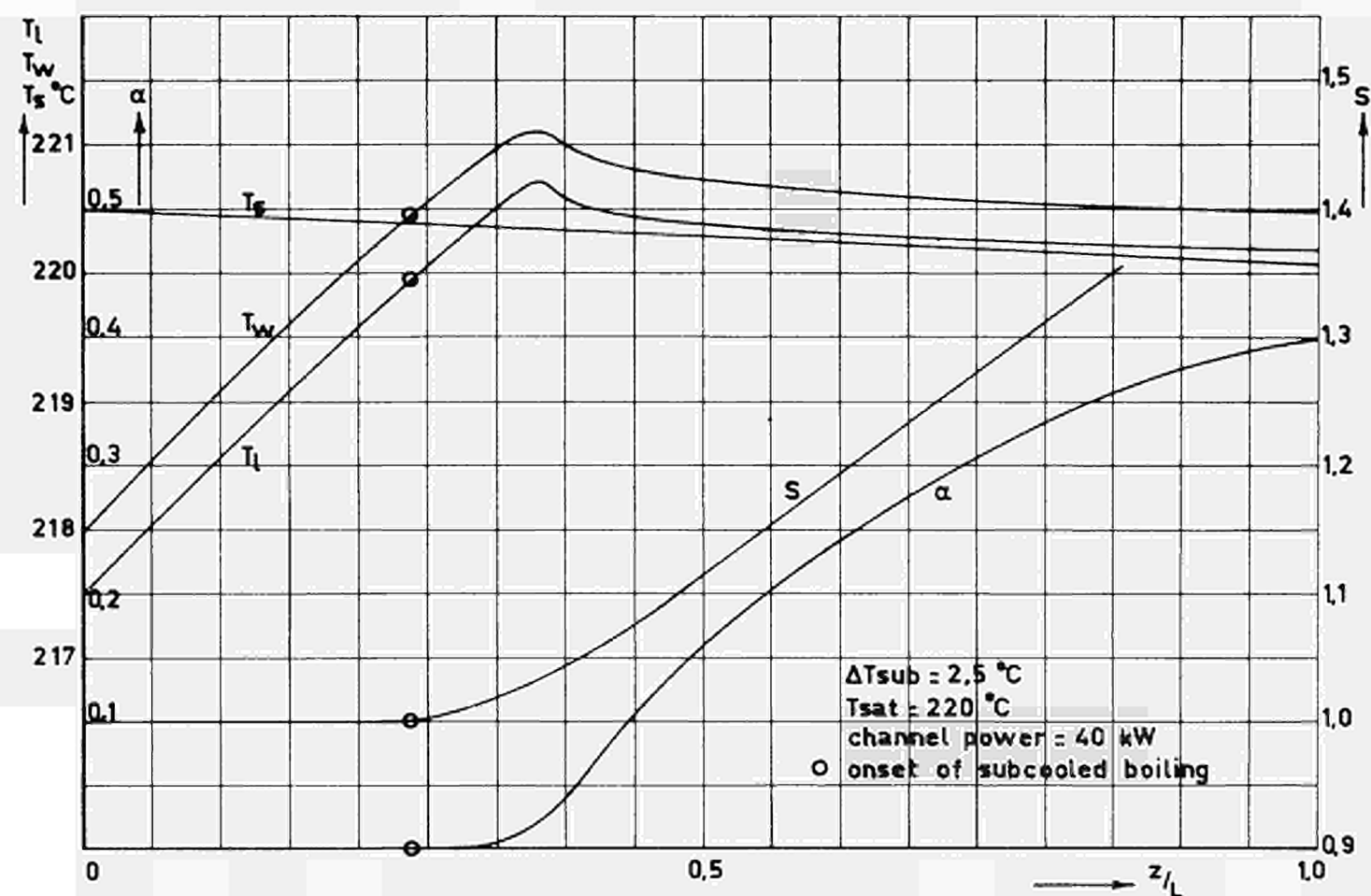


Fig. 23

Steady-state results calculated by a theoretical study based on "first principles".

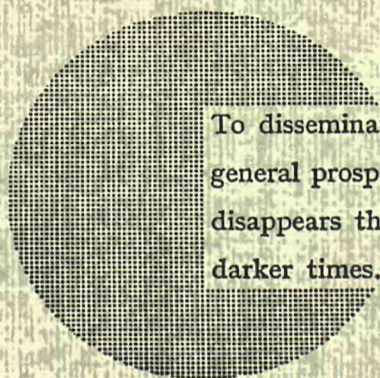
NOTICE TO THE READER

All Euratom reports are announced, as and when they are issued, in the monthly periodical **EURATOM INFORMATION**, edited by the Centre for Information and Documentation (CID). For subscription (1 year : US\$ 15, £ 6.5) or free specimen copies please write to :

Handelsblatt GmbH
"Euratom Information"
Postfach 1102
D-4 Düsseldorf (Germany)

or

Office central de vente des publications
des Communautés européennes
2, Place de Metz
Luxembourg



To disseminate knowledge is to disseminate prosperity — I mean general prosperity and not individual riches — and with prosperity disappears the greater part of the evil which is our heritage from darker times.

Alfred Nobel

SALES OFFICES

All Euratom reports are on sale at the offices listed below, at the prices given on the back of the front cover (when ordering, specify clearly the EUR number and the title of the report, which are shown on the front cover).

OFFICE CENTRAL DE VENTE DES PUBLICATIONS DES COMMUNAUTES EUROPEENNES

2, place de Metz, Luxembourg (Compte chèque postal N° 191-90)

BELGIQUE — BELGIË

MONITEUR BELGE
40-42, rue de Louvain - Bruxelles
BELGISCH STAATSBLAD
Leuvenseweg 40-42 - Brussel

LUXEMBOURG

OFFICE CENTRAL DE VENTE
DES PUBLICATIONS DES
COMMUNAUTES EUROPEENNES
9, rue Goethe - Luxembourg

DEUTSCHLAND

BUNDESANZEIGER
Postfach - Köln 1

NEDERLAND

STAATSDRUKKERIJ
Christoffel Plantijnstraat - Den Haag

FRANCE

SERVICE DE VENTE EN FRANCE
DES PUBLICATIONS DES
COMMUNAUTES EUROPEENNES
26, rue Desaix - Paris 15^e

ITALIA

LIBRERIA DELLO STATO
Piazza G. Verdi, 10 - Roma

UNITED KINGDOM

H. M. STATIONERY OFFICE
P. O. Box 569 - London S.E.1

EURATOM — C.I.D.
51-53, rue Belliard
Bruxelles (Belgique)

CDNA03789ENC